Physica D 481 (2025) 134850

Contents lists available at ScienceDirect

Physica D

journal homepage: www.elsevier.com/locate/physd

Stable spikes for a reaction–diffusion system modeling color pattern formation

Weiwei Ao [a], Juncheng Wei [b], Matthias Winter [c,*]

[a] Wuhan University, Department of Mathematics, Wuhan, 430072, China
[b] Chinese University of Hong Kong, Department of Mathematics, Hong Kong, China
[c] Brunel University of London, Department of Mathematics, UB8 3PH, Uxbridge, United Kingdom

ARTICLE INFO

Communicated by V.M. Perez-Garcia

MSC:
primary 35B35
92C15
secondary 35B40
92C37

Keywords:
Color pattern formation
Activator-inhibitor system
Stability
Steady states

ABSTRACT

We consider a reaction–diffusion system for color pattern formation with two activators and one inhibitor. Each of the activators models one of the colors being switched on, for example the first activator could represent the color blue and the second activator the color yellow. If both colors are present the pattern will have green color since the color green is achieved by a mixture of the colors blue and yellow. We prove rigorous results on the existence and stability of spikes for which one of the colors or both of them are switched on. To the best of our knowledge, this paper is the first study of spike solutions for a reaction–diffusion system with two activator and one inhibitor systems and arbitrary strength of the self-activation and cross-activation terms. We classify the different types of solutions which can exist depending on the choice of interaction parameters between the components and we show which of them are stable or unstable. In particular, solutions with spikes for both activators in the same position can be stable when cross-activation dominates over self-activation. On the other hand, solutions with a spike for only one activator and zero concentration for the other activator can be stable when self-activation dominates over cross-activation. The rigorous approach is based on analytical methods such as Green's function, Liapunov-Schmidt reduction and nonlocal eigenvalue problems. The analytical results are confirmed by numerical simulations.

1. Introduction

We study a reaction–diffusion system with two activators and one inhibitor modeling color pattern formation.

In this paper, we will prove the existence and study the stability of spike solutions for the system with two activators which display self-interaction and cross-interaction, coupled with one global inhibitor.

This system can be considered as a generalization of the standard two-component Gierer–Meinhardt system [1]

$$\begin{cases} u_t = \epsilon^2 u_{xx} - u + \dfrac{u^p}{v^q}, \\ \tau v_t = D v_{xx} - v + \dfrac{u^r}{v^s} \end{cases}$$

with exponents $(p, q, r, s) = (3, 1, 3, 0)$. Generally, it is assumed that the exponents (p, q, r, s) satisfy

$$p > 1, \quad q > 0, \quad r > 1, \quad s \geq 0, \text{ and } \frac{qr}{p-1} > s + 1.$$

(see [1]). Our choice of exponents satisfies these assumptions.

The t-indices indicate temporal derivatives and the x-indices indicate spatial derivatives. Here u is the activator, v is the inhibitor, $0 < \epsilon \ll 1$ and $D > 0$ are diffusion constants, and τ is a nonnegative time-relaxation constant.

The reaction–diffusion system considered in this paper is a system with two activators whose reaction kinetics has self-interaction of both activators and interaction of both activators with the inhibitor. In addition, the two activators have cross-interaction with each other.

* Corresponding author.
E-mail addresses: wwao@whu.edu.cn (W. Ao), wei@math.cuhk.edu.hk (J. Wei), matthias.winter@brunel.ac.uk (M. Winter).

https://doi.org/10.1016/j.physd.2025.134850
Received 10 December 2024; Received in revised form 5 May 2025; Accepted 17 July 2025
Available online 6 August 2025
0167-2789/© 2025 The Authors. Published by Elsevier B.V. This is an open access article under the CC BY license (http://creativecommons.org/licenses/by/4.0/).

We assume that the small diffusivities of the two activators are the same. We assume that the terms in the reaction kinetics are all cubic with respect to the activators.

All these assumptions can be relaxed. We will address this issue by presenting some more general numerical simulations (Section 6) and by discussing how the present study can be extended in future work (Section 7).

The activator-inhibitor system under investigation can be stated as follows:

$$\begin{cases} u_{1,t} = \epsilon^2 u_{1,xx} - u_1 + \dfrac{\mu_1 u_1^3 + \beta u_1 u_2^2}{v}, \quad u_{2,t} = \epsilon^2 u_{2,xx} - u_2 + \dfrac{\mu_2 u_2^3 + \beta u_1^2 u_2}{v}, \\ \tau v_t = D v_{xx} - v + \mu_1 u_1^3 + \beta u_1 u_2^2 + \mu_2 u_2^3 + \beta u_1^2 u_2. \end{cases} \tag{1.1}$$

Here $0 < \epsilon \ll 1$ and $D > 0$ are diffusion and τ is a nonnegative time-relaxation constant as in the standard Gierer–Meinhardt system. Further, μ_1, μ_2, $\beta > 0$ are positive constants for the self- and cross-activation of the activators, respectively.

The positive constants μ_1, μ_2 model the strength of self-activation of each activator and β represents the strength of cross-activation.

By rescaling the amplitudes of u_1 and u_2 we can always achieve that the mixed terms have the same coefficient β, so we can make this assumption without loss of generality.

We will derive results for the system (1.2) on a bounded interval $\Omega = (-L, L)$ for $L > 0$ with Neumann boundary conditions. We classify the different types of solutions which can exist depending on the choice of interaction parameters between the components and we show which of them are stable or unstable. In particular, solutions with spikes for both activators in the same position can be stable when cross-activation dominates over self-activation. On the other hand, solutions with a spike for only one activator and zero concentration for the other activator can be stable when self-activation dominates over cross-activation.

Many mechanisms can play a role for color pattern formation. For a recent survey we refer to [2]. Reaction–diffusion systems of activator-inhibitor type can model the first stage of pattern formation by self-organization. The maxima of the activator peaks can trigger differentiation on the cellular level leading to the implementation of the final pattern. Two activators will be able to stimulate two different cellular processes which can lead to the formation of patterns with two different colors. Each of the activators models one of the colors being switched on, for example the first activator could represent the color blue and the second activator the color yellow. If both colors are present the pattern will have green color since the color green is achieved by a mixture of the colors blue and yellow. We prove rigorous results on the existence and stability of spikes for which one of the colors or both of them are switched on.

Understanding the properties of the reaction–diffusion system and its solutions can give insight into formation of patterns which arise without prepatterns or external information but purely through a self-contained process. The model is motivated by phenomenological considerations rather than a mechanistic derivation.

We would like to comment on some of the cellular processes behind color pattern formation. Certain pigment-containing cells called chromatophores are responsible for the coloring in the skins of reptiles, amphibians, and fish. Color patterns result from the spatial variation in the types, properties, and spatial arrangements of chromatophores.

In zebrafish the chromatophores are the pigment cells melanophores (black/brown color), iridophores (iridescent, color depends on viewing angle), and xanthophores (yellow). Recent molecular genetic studies have shown that interactions between the pigment cells play major roles in pattern formation [3,4]. The color for chameleons can be changed through active tuning of a lattice of guanine nanocrystals, a frequent type of organic biocrystal associated with animal coloring, inside a skin layer of iridophores. This has been confirmed by using osmotic pressure experiments and theoretical optical modeling [5].

Stripes in zebrafish have been modeled using an agent-based approach [6]. It has been shown that iridophores can act as a stabilizer of zebrafish stripes [7]. Topological analysis of zebrafish patterns has been performed in [8].

To the best of our knowledge, this paper is the first study of spike solutions for a reaction–diffusion system with two activator and one inhibitor systems and arbitrary strength of the self-activation and cross-activation terms.

Let us make some comments on previous publications related to the current study. We will put the system and the results in context and justify their novelty.

Recently results on spike solutions have been established in a related reaction–diffusion system modeling competition between two plant species with different rates of water intake [9]. This system is based on reaction kinetics of Klausmeier type with two activators and one inhibitor. The activators display self-interaction and interaction with the inhibitor, but there is no cross-interaction between the two activators. The authors study spike solutions for which one of the two activators is positive at a certain location but not both of them. Spike solutions for which the two activators are identical also exist for this system but they are expected to be unstable due to the absence of activator cross-interaction.

Spike solutions for other large reaction–diffusion systems with more than two components have been studied before, including the hypercycle of Eigen and Schuster [10–12] or mutual exclusion of spikes [13].

The reaction–diffusion model for color pattern formation is similar to the hypercycle of Eigen and Schuster [14] but with different interactions between activators. For the hypercycle, there is only activator interaction with nearest neighbors, the interaction is not symmetric and there is no self-interaction. The hypercycle can have an arbitrary number of activators. In the special case of two activators the main difference is the absence of self-interaction terms which are considered in this paper.

Mutual exclusion of spikes is modeled by a five-component Meinhardt–Gierer model for mutually exclusive patterns and segmentation [15,16]. The overall feedback mechanism of the system can be summarized as follows: Nonlocal activation is coupled with self-activation and overall inhibition. The spikes for the two activators are located in different positions, whereas in the current study the two activators can co-exist in the same location.

Finally, our model is related to Schrödinger systems. The activator interaction in our system is a special case of the interaction for Schrödinger systems. Our model can be derived by adding an inhibitor component to a Schrödinger system. For Schrödinger systems, the existence and Morse index of spike solutions have been studied extensively by Wei and Lin, see [17–22] and references therein. The uniqueness of positive ground states has been shown in [23] and the nondegeneracy of ground states has been proved in [24], while the Morse indices of ground state solutions for Schrödinger systems with an arbitrary number of components have been considered in [25]. For Schrödinger systems without inhibitor the type of solutions considered in our paper are unstable with Morse index 1 or 2. Due to the presence of the inhibitor, it is possible to stabilize some of these solutions.

We rescale the unknown functions as follows to achieve amplitudes of order $O(1)$:

$$\hat{u}_1(x) = \epsilon u_1(x), \quad \hat{u}_2(x) = \epsilon u_2(x), \quad \hat{v}(x) = \epsilon^2 v(x).$$

In terms of the rescaled functions, the system can be restated as follows:

$$\begin{cases} \hat{u}_{1,t} = \epsilon^2 \hat{u}_{1,xx} - \hat{u}_1 + \dfrac{\mu_1 \hat{u}_1^3 + \beta \hat{u}_1 \hat{u}_2^2}{\hat{v}}, \quad \hat{u}_{2,t} = \epsilon^2 \hat{u}_{2,xx} - \hat{u}_2 + \dfrac{\mu_2 \hat{u}_2^3 + \beta \hat{u}_1^2 \hat{u}_2}{\hat{v}}, \\ \tau \hat{v}_t = D\hat{v}_{xx} - \hat{v} + \left(\mu_1 \hat{u}_1^3 + \beta \hat{u}_1 \hat{u}_2^2 + \mu_2 \hat{u}_2^3 + \beta \hat{u}_1^2 \hat{u}_2\right) \epsilon^{-1}. \end{cases} \tag{1.2}$$

It is known that these patterns are unstable without inhibitor (see for example [24–26]). In fact, without inhibitor, the Morse index of a single spike solution will be 1 or 2, depending on the region in the β-μ parameter space, which we refer to below as the β-μ condition. Here we will show that with global inhibition it is possible to get stable spiky patterns. Depending on the β-μ condition, at a certain location either both activators can have a spike forming a local pattern, or only one of the activators has a spike and the other activator zero values. Both of these types of solutions can be stable or unstable, depending on the β-μ condition.

The system (1.2) is similar to a hypercycle with cubic terms and two activators, and Gierer–Meinhardt kinetics instead of Gray-Scott kinetics, see [11]. For the study of spiky solutions of the hypercycle with quadratic interaction terms we refer the readers to [10,12].

We recall that the classical Gierer–Meinhardt system as well as the three-component system considered here are both Turing systems [27] as they allow spatial patterns to arise out of a homogeneous steady state by the so-called Turing instability. Some analytical results for the existence and stability of spiky Turing pattern for the Gierer–Meinhardt system have been obtained for example in [28–35]. The results have been reviewed in [36].

Next we are going to state the rigorous results on the existence and stability of stationary spiky patterns for the system (1.2).

We prove the **existence** of three types of spiky pattern solutions:

A solution of Type 1 which has a spike for u_1 and spike for u_2, both located at zero.

A solution of Type 2 which has a spike for u_1 located at zero and $u_2 = 0$.

A solutions of Type 3 which has a spike for u_2 located at zero and $u_1 = 0$.

The spikes for u_1 and u_2 in a solution of Type 1 have the same profile except for possibly their amplitudes. To determine the amplitudes of the activator spikes we have to solve a system which depends on the coefficients of the reaction terms of the self-interaction and cross-interaction of activators. We will see that these amplitudes depend on the size of inhibitor and for larger inhibitor we need larger activator amplitudes to balance the interaction (as in the classical Gierer–Meinhardt system).

Let $w(y)$ be the unique positive and even homoclinic solution of the equation

$$w_{yy} - w + w^3 = 0 \tag{1.3}$$

on the real line decaying to zero at $\pm\infty$. Let $H^2_{N,ev}(-L, L)$ be the space of functions in $H^2(-L, L)$ which satisfy Neumann boundary conditions and are even.

The main results are as follows:

We first have the existence of Type 1 solutions with a spike for u_1 and u_2.

Theorem 1. *Assume that $\epsilon > 0$ is small enough and*

$$\beta > \max(\mu_1, \mu_2) \text{ or } \beta < \min(\mu_1, \mu_2).$$

Then there exist spiky steady states to (1.2) in $H^2_{N,ev}(-L, L)$ such that

$$u_1^\epsilon(x) = t_1 \sqrt{v_\epsilon(0)} w\left(\frac{x}{\epsilon}\right) \chi(x)(1 + O(\epsilon)), \quad u_2^\epsilon(x) = t_2 \sqrt{v_\epsilon(0)} w\left(\frac{x}{\epsilon}\right) \chi(x)(1 + O(\epsilon)) \tag{1.4}$$

where $t_i > 0$ is a constant which satisfies (2.10), $v_\epsilon(0)$ is given by (2.11) and $\chi(x)$ is a cutoff function defined in (3.1).

Similarly, we can show the existence of Type 2 solutions with a spike for u_1 and $u_2 = 0$.

Theorem 2. *Assume that $\epsilon > 0$ is small enough and $\beta \neq \mu_1$. Then there exist spiky steady states to (1.2) in $H^2_{N,ev}(-L, L)$ such that*

$$u_1^\epsilon(x) = t_1 \sqrt{v_\epsilon(0)} w\left(\frac{x}{\epsilon}\right) \chi(x)(1 + O(\epsilon)), \quad u_2^\epsilon(x) = 0, \tag{1.5}$$

where $t_1 = \frac{1}{\sqrt{\mu_1}}$, $v_\epsilon(0)$ is given by (2.15) and $\chi(x)$ is a cutoff function defined in (3.1).

Remark 1. By symmetry, Theorem 2 is still valid if u_1 is swapped with u_2 and μ_1 is swapped with μ_2, which implies the existence of Type 3 spike solutions when $\beta \neq \mu_2$.

The stability properties of the spiky solutions are as follows:

Theorem 3. *The steady states to (1.2) given in Theorem 1 are linearly stable if $\beta > \max(\mu_1, \mu_2)$. They are linearly unstable if $\beta < \min(\mu_1, \mu_2)$.*

Theorem 4. *The steady states to (1.2) given in Theorem 2 are linearly stable if $\beta < \mu_1$. They are linearly unstable if $\beta > \mu_1$.*

Remark 2. For $\mu_1 < \beta < \mu_2$ the solution with $u_1 \neq 0$ and $u_2 \neq 0$ does not exist, in the same way as for Schrödinger systems without v component, see [23].

Remark 3. In case $\mu_1 < \mu_2$ there is a transcritical bifurcation at $\beta = \mu_1$ and $\beta = \mu_2$, respectively. For $\beta = \mu_1$ there is a bifurcation of the Type 1 solution from the Type 2 solution, and for $\beta = \mu_2$ there is a bifurcation of the Type 1 solution from the Type 3 solution.

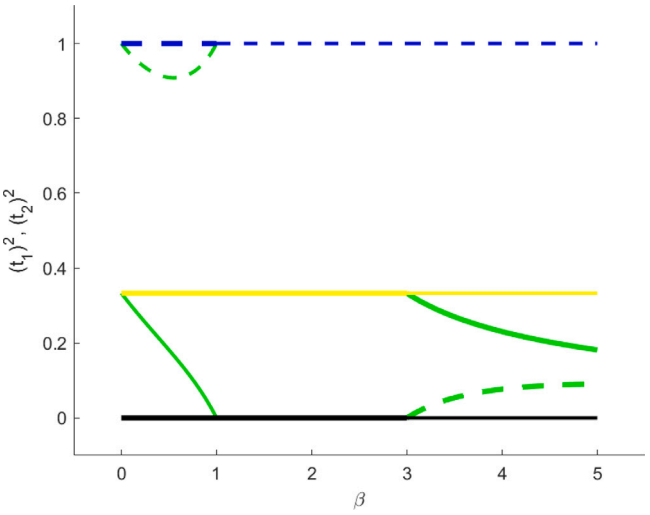

Fig. 1. Bifurcation diagram of single spike solutions with parameters $\mu_1 = 1$, $\mu_2 = 3$ and bifurcation parameter β; dashed lines represent t_1^2, solid lines represent t_2^2; thick lines indicate stable solutions, thin lines indicate unstable solutions.

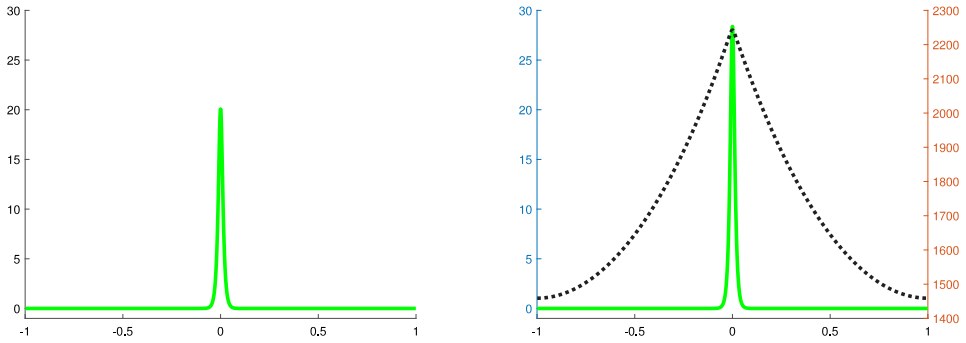

Fig. 2. Type 1 solution ($u_1 > 0$, $u_2 > 0$), color green, single spike, $\epsilon^2 = 0.0001$, $D = 1$, $\mu_1 = 1$, $\mu_2 = 3$, $\beta = 5$.

We display the solutions in a bifurcation diagram (see Fig. 1).

What do these mathematical results tell us about biological applications? The two activators u_1 and u_2 can represent different colors in the living organism. For example, u_1 can represent the color blue and u_2 the color yellow. Then a spike with only u_1 positive indicates a blue spot and a spike with only u_2 positive indicates a yellow spot. Finally, a spike with both u_1 and u_2 positive represents a green spot since the color green is achieved by a mixture of the colors blue and yellow.

To summarize, suppose $\beta < \mu_1 < \mu_2$. Then Type 1 solutions are unstable, Type 2 and 3 solutions are stable. Stable patterns can have blue spots or yellow spots. Green spots are possible but they are unstable.

For $\mu_1 < \beta < \mu_2$, Type 1 solutions do not exist. Type 3 solutions are stable and Type 2 solutions are unstable. Stable patterns can have yellow spots. Blue spots are possible but they are unstable. Green spots are impossible.

For $\mu_1 < \mu_2 < \beta$, Type 1 solutions are stable, whereas both Type 2 and 3 solutions are unstable. Stable patterns can have green spots. Blue spots or yellow spots are possible but they are unstable.

We present numerical simulations of the three types of solutions. The first subfigure always shows u_1 (solid line), the second subfigure shows u_2 (left axis, solid line) and v (right axis, dotted line). We will discuss more details about the numerical simulations in Section 6 (see Figs. 2–4).

Remark 4. By choosing the parameters suitably it is possible to achieve **stable Type 1 solutions with any proportion of mixing** between blue and yellow color. We can see this as follows: We first compute

$$\frac{t_2}{t_1} = \sqrt{\frac{\beta - \mu_1}{\beta - \mu_2}}.$$

Therefore, varying parameters in the range $\mu_1 < \mu_2 < \beta$ we can get any ratio for t_2/t_1 in the interval

$$1 < \frac{t_2}{t_1} < \infty$$

and varying parameters in the range $\mu_2 < \mu_1 < \beta$ we can get any ratio for t_2/t_1 in the interval

$$0 < \frac{t_2}{t_1} < 1.$$

(Note that we can keep μ_1 and μ_2 fixed and vary β accordingly.)

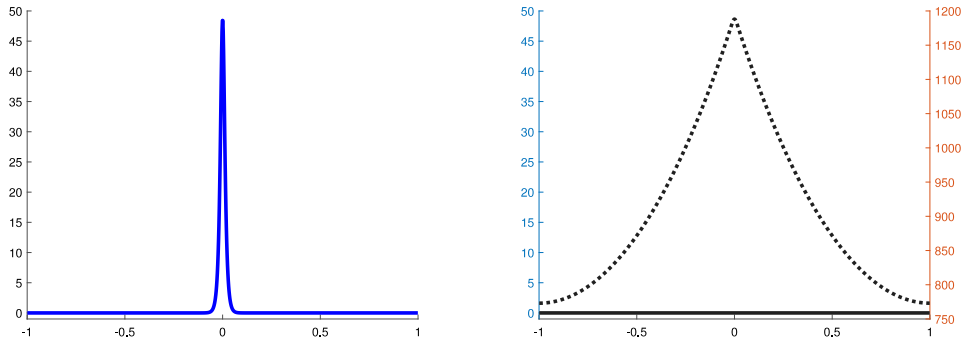

Fig. 3. Type 2 solution ($u_1 > 0$, $u_2 = 0$), color blue, single spike, $\epsilon^2 = 0.0001$, $D = 1$, $\mu_1 = 1$, $\mu_2 = 3$, $\beta = 0.5$.

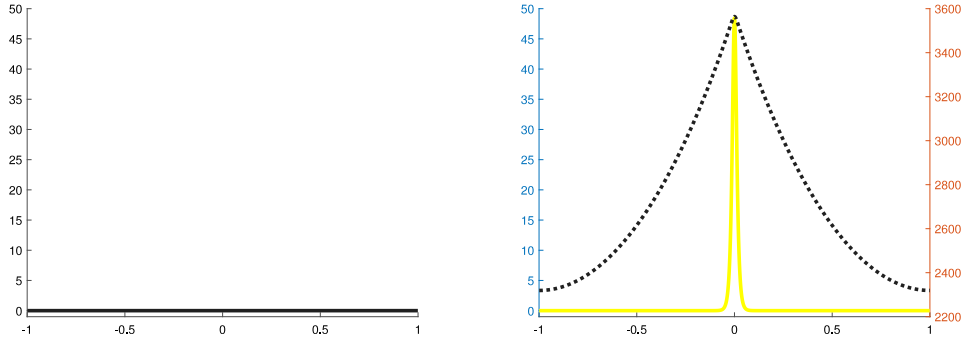

Fig. 4. Type 3 solution ($u_1 = 0$, $u_2 > 0$), color yellow, single spike, $\epsilon^2 = 0.0001$, $D = 1$, $\mu_1 = 1$, $\mu_2 = 3$, $\beta = 2$.

Choosing $\mu_1 = \mu_2$ we get $t_1 = t_2$ and so $\frac{t_2}{t_1} = 1$. (If we keep μ fixed and vary β then we get $\frac{t_2}{t_1} = 1$ for any β.)
In summary, we can achieve any value for $\frac{t_2}{t_1}$ in the range

$$0 < \frac{t_2}{t_1} < \infty.$$

Remark 5. The results can be generalized to the case of negative parameters. For the existence of Type 1 solutions, we need $\max(\mu_1, \mu_2) < \beta$ or $\beta < \min(\mu_1, \mu_2)$.

If β is negative, then μ_1 and μ_2 must both be positive, otherwise (2.3) is not possible. Thus we need to have $\beta < 0 < \min(\mu_1, \mu_2)$. To satisfy (2.10), it is further required that $\beta > -\sqrt{\mu_1\mu_2}$. In summary, we need $-\sqrt{\mu_1\mu_2} < \beta < 0 < \min(\mu_1, \mu_2)$. Under this assumption, a Type 1 solution exists. We have $g(\beta) < 0$, and so the solution is unstable.

If μ_1 is negative, then by (2.3), β must be positive and so $\beta - \mu_1 > 0$. From (2.10), we get $\beta^2 - \mu_1\mu_2 > 0$ and $\beta - \mu_2 > 0$. This implies $\frac{\beta^2}{\mu_1} < \mu_2 < \beta$. Note that μ_2 can have either sign. Under these conditions a Type 1 solution exists. Here $g(\beta) > 0$, and so the solution is stable.

For $\beta < 0$ and $\mu_1 > 0$, Type 2 solutions exist and they are stable. Analogously, for $\beta < 0$ and $\mu_2 > 0$, Type 3 solutions exist and they are stable.

The paper is organized as follows: In Section 2, we compute the amplitudes of spikes. In Section 3, we show the existence of solutions. In Section 4, we first derive the eigenvalue problem. Then we compute the large (i.e. $O(1)$) eigenvalues and we derive sufficient conditions for the stability of solutions with respect to these. In Section 5, we consider the small (i.e. $o(1)$) eigenvalues. We outline how to rigorously compute them to leading order and state the main criterion on the stability of solutions with respect to small eigenvalues. Sufficient conditions for this stability are derived. In Section 6, we present some numerical simulations of spike solutions which are more general than the analytical results. In Section 7, we discuss our results and give an outlook. In the Appendix, results from previous publications are provided which are used repeatedly in the paper.

2. Computing the amplitudes

In this section, we will consider spiky steady states of (1.2) of the following three types:
Type 1: spike for u_1 and spike for u_2, both located at zero,
Type 2: spike for u_1 located at zero and $u_2 = 0$.
Type 3: spike for u_2 located at zero and $u_1 = 0$.
Since Type 3 is symmetric to Type 2 by inter-changing u_1 and u_2, and μ_1 and μ_2, we will only consider Type 1 and Type 2 solutions.
We first construct steady states of the form

$$u_1(x) = t_1\sqrt{v_\epsilon(0)}w\left(\frac{x}{\epsilon}\right)(1 + O(\epsilon)), \quad u_2(x) = t_2\sqrt{v_\epsilon(0)}w\left(\frac{x}{\epsilon}\right)(1 + O(\epsilon)), \tag{2.1}$$

where $w(y)$ is the unique positive and even homoclinic solution of the equation

$$w_{yy} - w + w^3 = 0 \tag{2.2}$$

on the real line decaying to zero at $\pm\infty$. We will compute $v_\epsilon(0)$, t_1, t_2. The result will be stated in Lemma 1.

From the first two equations to (1.2), we will choose t_1 and t_2 such that

$$\mu_1 t_1^2 + \beta t_2^2 = 1,\ \mu_2 t_2^2 + \beta t_1^2 = 1. \tag{2.3}$$

All functions used throughout the paper belong to the Hilbert space $H^2(-L, L)$ and the error terms are taken in the norm $H^2(-L, L)$ unless otherwise stated. After integrating (1.3) over $\mathbb{R}$, we get the relation

$$\int_{\mathbb{R}} w(y)\,dy = \int_{\mathbb{R}} w^3(y)\,dy \tag{2.4}$$

which will be used frequently, often without explicitly stating it.

Note that u_1 and u_2 are spatially small-scale variables, as $\epsilon \ll 1$, and v_ϵ is a spatially large-scale variable. For steady states, using Green's functions, the slow variable v, to leading order, can be expressed by an integral representation.

To get this representation, by (2.1) the nonlinear terms in the last equation of (1.2) can be expanded as

$$\mu_1 u_1^3(x) + \beta u_1(x) u_2^2(x) = t_1\,(v_\epsilon(0))^{3/2}\,\epsilon \left(\int_{\mathbb{R}} w^3\right) \delta_0(x) + O(\epsilon^2),$$

$$\mu_2 u_2^3(x) + \beta u_1^2(x) u_2(x) = t_2\,(v_\epsilon(0))^{3/2}\,\epsilon \left(\int_{\mathbb{R}} w^3\right) \delta_0(x) + O(\epsilon^2),$$

where $\delta_0(x)$ is the Dirac delta distribution centered at 0.

Using the Green's function $G_D(x, y)$ which is defined as the unique solution of the equation

$$D\Delta G_D(x, y) - G_D(x, y) + \delta_y(x) = 0, \quad -L < x < L, \quad G_{D,x}(-L, y) = G_{D,x}(L, y) = 0, \tag{2.5}$$

we can represent $v_\epsilon(x)$ by using the third equation of (1.2) as

$$v_\epsilon(x) = (t_1 + t_2)(v_\epsilon(0))^{3/2} \left(\int_{\mathbb{R}} w^3(y) dy\right) G_D(x, 0) + O(\epsilon). \tag{2.6}$$

An elementary calculation gives

$$G_D(x, y) = \begin{cases} \frac{\theta}{\sinh(2\theta L)} \cosh\theta(L + x)\cosh\theta(L - y), & -L < x < y < L, \\ \frac{\theta}{\sinh(2\theta L)} \cosh\theta(L - x)\cosh\theta(L + y), & -L < y < x < L \end{cases} \tag{2.7}$$

with $\theta = 1/\sqrt{D}$. Note that

$$G_D(x, y) = \frac{1}{2\sqrt{D}} e^{-|x-y|/\sqrt{D}} - H_D(x, y), \tag{2.8}$$

where H_D is the regular part of the Green's function G_D. In particular, for $L = \infty$, we have

$$G_D(x, y) = \frac{1}{2\sqrt{D}} e^{-|x-y|/\sqrt{D}} =: K_D(x, y). \tag{2.9}$$

We first compute t_1 and t_2 from (2.3). Considering (2.3) as a linear system with the unknowns t_1^2 and t_2^2, we get

$$t_1^2 = \frac{\beta - \mu_2}{\beta^2 - \mu_1\mu_2}, \quad t_2^2 = \frac{\beta - \mu_1}{\beta^2 - \mu_1\mu_2}. \tag{2.10}$$

It remains to derive $v_\epsilon(0)$. From (2.6), for $x = 0$ we get

$$v_\epsilon(0) = (v_\epsilon(0))^{3/2}(t_1 + t_2) G_D(0, 0) \left(\int_{\mathbb{R}} w^3(y) dy\right) + O(\epsilon).$$

This implies

$$v_\epsilon(0) = \frac{1}{G_D(0, 0)^2 (t_1 + t_2)^2 \left(\int_{\mathbb{R}} w^3\right)^2} + O(\epsilon). \tag{2.11}$$

In the following, we state the first main result of this section on the amplitudes of Type 1 solutions:

Lemma 1. *Assume that $\epsilon > 0$ is small enough and*

$$\beta > \max(\mu_1, \mu_2) \text{ or } \beta < \min(\mu_1, \mu_2).$$

We consider spike solutions of (1.2) of the type

$$u_1(x) = t_1 \sqrt{v_\epsilon(0)} w\left(\frac{x}{\epsilon}\right)(1 + O(\epsilon)), \quad u_2(x) = t_2 \sqrt{v_\epsilon(0)} w\left(\frac{x}{\epsilon}\right)(1 + O(\epsilon)),$$

where $w(y)$ is the unique solution of (2.2). Then the amplitudes t_1 and t_2 are given by (2.10), $v_\epsilon(0)$ satisfies (2.11), and the Green's function G_D is defined in (2.5).

Next, we consider the Type 2 spike solutions. We will construct solutions of the form

$$u_1(x) = t_1 \sqrt{v_\epsilon(0)} w\left(\frac{x}{\epsilon}\right)(1 + O(\epsilon)), \quad u_2(x) = 0. \tag{2.12}$$

We will compute $v_\epsilon(0)$ and t_1. The result will be stated in Lemma 2.

From the first equation of (1.2), we get in leading order

$$t_1 = \mu_1 t_1^3$$

which implies

$$t_1 = \frac{1}{\sqrt{\mu_1}}. \tag{2.13}$$

From the third equation of (1.2), we get

$$v_\epsilon(x) = t_1 (v_\epsilon(0))^{3/2} \left(\int_{\mathbb{R}} w^3 \right) G_D(x,0) + O(\epsilon). \tag{2.14}$$

From (2.14), for $x = 0$ we get

$$v_\epsilon(0) = (v_\epsilon(0))^{3/2} t_1 G_D(0,0) \left(\int_{\mathbb{R}} w^3 \right) + O(\epsilon).$$

Together with (2.13) this implies

$$v_\epsilon(0) = \frac{1}{G_D(0,0)^2 t_1^2 \left(\int_{\mathbb{R}} w^3 \right)^2} + O(\epsilon). \tag{2.15}$$

With these in hand, we finally state the second main result of this section on the amplitude of Type 2 spike solutions:

Lemma 2. *Assume that $\epsilon > 0$ is small enough. We consider spike solutions of (1.2) of the type*

$$u_1(x) = t_1 \sqrt{v_\epsilon(0)} w\left(\frac{x}{\epsilon}\right)(1 + O(\epsilon)), \quad u_2(x) = 0,$$

where $w(y)$ is the unique solution of (2.2). Then the amplitude t_1 is given by (2.13), and $v_\epsilon(0)$ satisfies (2.15), where the Green's function G_D is defined in (2.5).

3. Existence of spike solutions

In this section, we use the contraction mapping principle to rigorously prove the existence of spiky solutions.

The issue to handle here is that the linear operator obtained by the linearization of system (1.2) around (2.1) has a nontrivial approximate kernel. This comes from the fact that taking a derivative of Eq. (2.2) with respect to y implies

$$(w_y)_{yy} - w_y + 3w^2 w_y = 0.$$

Thus, w_y belongs to the kernel of the linearization of (2.2) around w. Note that the function w_y represents the translation mode of w. To eliminate the approximate kernel from the function space we will construct solutions in spaces of even functions. Since the approximate kernel consists of odd functions, we will be able to show in this section first that the linear operator restricted to even functions is uniformly invertible for ϵ small enough. Using this result, we can then complete the proof.

Recall that for given $u_1, u_2 \in H^2_N(\Omega_\epsilon)$, where $\Omega_\epsilon = (-L/\epsilon, L/\epsilon)$ and $H^2_N(\Omega_\epsilon)$ denotes the space of all functions in $H^2(\Omega_\epsilon)$ satisfying Neumann boundary conditions, since the third equation of (1.2) is linear in v, the inhibitor v is uniquely determined for given u_1, u_2. Therefore, the steady state problem can be reduced to solving the first two equations.

We are looking for solutions which satisfy

$$u_1(x) = t_1 \sqrt{v_\epsilon(0)} w\left(\frac{x}{\epsilon}\right) \chi(x)(1 + O(\epsilon)), \quad u_2(x) = t_1 \sqrt{v_\epsilon(0)} w\left(\frac{x}{\epsilon}\right) \chi(x)(1 + O(\epsilon))$$

which are even functions, i.e. $u_i(x) = u_i(-x)$, $i = 1, 2$. To this end, we assume that χ is a smooth and even cut-off function such that

$$\chi(x) = 1 \text{ for } |x| \le L/3$$

and

$$\chi(x) = 0 \text{ for } |x| \ge 2L/3. \tag{3.1}$$

To construct a solution which consists of even functions we will be working in Sobolev spaces of even functions.

We are now going to derive a solution by using the contraction mapping principle. Denoting the r.h.s. of the first two equation of (1.2) by

$$S_\epsilon[t_1 \sqrt{v_\epsilon(0)} w\chi + a_1, t_2 \sqrt{v_\epsilon(0)} w\chi + a_2],$$

our problem can be re-written as follows: Find a_1 and a_2 such that

$$S_\epsilon[t_1 \sqrt{v_\epsilon(0)} w\chi + a_1, t_2 \sqrt{v_\epsilon(0)} w\chi + a_2] = 0,$$

where

$$S_\epsilon : (H^2_{N,ev}(\Omega_\epsilon))^2 \to (L^2_{ev}(\Omega_\epsilon))^2.$$

Here the index "ev" stands for the restriction of the function spaces to even functions, i.e.

$$L^2_{ev}(\Omega_\epsilon) = \{u \in L^2(\Omega_\epsilon),\ u(y) = u(-y) \text{ for all } y \in \Omega_\epsilon\},$$

$$H^2_{N,ev}(\Omega_\epsilon) = \{u \in H^2_N(\Omega_\epsilon),\ u(y) = u(-y) \text{ for all } y \in \Omega_\epsilon\}.$$

To this end, we need to study the linearized operator

$$L_\epsilon : (H^2_{N,ev}(\Omega_\epsilon))^2 \to (L^2(\Omega_\epsilon))^2$$

defined by

$$L_\epsilon \phi := DS_\epsilon[t_1 \sqrt{v_\epsilon(0)} w\chi, t_2 \sqrt{v_\epsilon(0)} w\chi]\phi,$$

where $DS_\epsilon[\cdot]$ denotes the Fréchet derivative of the operator S_ϵ at $(t_1\sqrt{v_\epsilon(0)}w\chi, t_2\sqrt{v_\epsilon(0)}w\chi)^T$.

Then we have the following key result about the uniform invertibility of the linearized operator L_ϵ. The proof is quite standard and it is based on computing the kernel of the limiting operator as $\epsilon \to 0$. We outline the key steps of the argument. The last part of the argument is specific to the system considered in this paper.

Proposition 1. *There exist positive constants $\bar\epsilon$, c such that we have for all $\epsilon \in (0, \bar\epsilon)$,*

$$\|L_\epsilon\phi\|_{L^2(\Omega_\epsilon)} \geq c\,\|\phi\|_{H^2(\Omega_\epsilon)} \quad \textit{for all} \quad \phi = (\phi_1, \phi_2)^T \in (H^2_{N,ev}(\Omega_\epsilon))^2. \tag{3.2}$$

Further, the linear mapping L_ϵ is surjective.

Proof. We prove by contradiction. Suppose that (3.2) is false. Then there exist sequences $\{\epsilon_k\}$, $\{\phi^k\}$ with $\epsilon_k \to 0$, $\phi^k = \phi_{\epsilon_k} \in (H^2_{N,ev}(\Omega_\epsilon))^2$, $k = 1, 2, \dots$ such that

$$\|L_{\epsilon_k}\phi^k\|_{(L^2(\Omega_{\epsilon_k}))^2} \to 0, \quad \text{as } k \to \infty, \quad \|\phi^k\|_{(H^2(\Omega_{\epsilon_k}))^2} = 1, \quad k = 1, 2, \dots . \tag{3.3}$$

At first (after rescaling) ϕ_{ϵ_k} is only defined on Ω_{ϵ_k}. However, by a standard result (compare [37]) it can be extended to $\mathbb{R}$ such that its norm in $H^2(\mathbb{R})$ is still bounded by a constant independent of ϵ_k for ϵ_k small enough. It is then a standard procedure to show that this extension converges strongly in $H^2(\Omega_\epsilon)$ to some limit ϕ_∞ with $\|\phi_\infty\|_{(H^2(\mathbb{R}))^2} = 1$. For the functional-analytic details of the argument, we refer to [38].

Then $\phi_\infty = (\phi_1, \phi_2)^T$ solves the system

$$\begin{aligned}&\Delta\phi_1 - \phi_1 + [(2\mu_1 t_1^2 + 1)\phi_1 + 2\beta t_1 t_2 \phi_2]w^2 \\ &\quad - \frac{t_1}{t_1 + t_2}\left[(2\mu_1 t_1^2 + 1 + 2\beta t_1 t_2)\int_{\mathbb{R}} w^2\phi_1\,dy + (2\mu_2 t_2^2 + 1 + 2\beta t_1 t_2)\int_{\mathbb{R}} w^2\phi_2\,dy\right]\frac{w^3}{\int_{\mathbb{R}} w^3\,dy} = 0,\end{aligned} \tag{3.4}$$

$$\begin{aligned}&\Delta\phi_2 - \phi_2 + [(2\mu_2 t_2^2 + 1)\phi_2 + 2\beta t_1 t_2 \phi_1]w^2 \\ &\quad - \frac{t_2}{t_1 + t_2}\left[(2\mu_2 t_2^2 + 1 + 2\beta t_1 t_2)\int_{\mathbb{R}} w^2\phi_2\,dy + (2\mu_1 t_1^2 + 1 + 2\beta t_1 t_2)\int_{\mathbb{R}} w^2\phi_1\,dy\right]\frac{w^3}{\int_{\mathbb{R}} w^3\,dy} = 0.\end{aligned} \tag{3.5}$$

This system is the special case with $\lambda = 0$ of (4.5) and (4.6) derived in Section 4. To avoid repetition of the derivations we refer to Section 4, where the derivation will be made in a more general case.

Next we prove $\phi_1 = \phi_2 = 0$. This can be done using similar arguments as in Section 4, by first showing that $-t_2\phi_1 + t_1\phi_2 = 0$, and then that $t_1\phi_1 + t_2\phi_2 = 0$. Thus, $\phi_1 = \phi_2 = 0$. To avoid repetition, here we refer to the detailed calculations given below in the proof of Proposition 2.

This contradicts the assumption $\|\phi\|_{H^2(\Omega_\epsilon)} = 1$. Therefore, (3.2) must be true.

In order to show its surjectivity, we need to show that the kernel of the adjoint operator is trivial, namely that the following system has only the zero solution $\phi = (\phi_1, \phi_2)^T$:

$$\begin{aligned}&\Delta\phi_1 - \phi_1 + [(2\mu_1 t_1^2 + 1)\phi_1 + 2\beta t_1 t_2 \phi_2]w^2 \\ &\quad - \frac{2\mu_1 t_1^2 + 1 + 2\beta t_1 t_2}{t_1 + t_2}\left[t_1\int_{\mathbb{R}} w^3\phi_1\,dy + t_2\int_{\mathbb{R}} w^3\phi_2\,dy\right]\frac{w^2}{\int_{\mathbb{R}} w^3\,dy} = 0,\end{aligned} \tag{3.6}$$

$$\begin{aligned}&\Delta\phi_2 - \phi_2 + [(2\mu_2 t_2^2 + 1)\phi_2 + 2\beta t_1 t_2 \phi_1]w^2 \\ &\quad - \frac{2\mu_2 t_2^2 + 1 + 2\beta t_1 t_2}{t_1 + t_2}\left[t_2\int_{\mathbb{R}} w^3\phi_2\,dy + t_1\int_{\mathbb{R}} w^3\phi_1\,dy\right]\frac{w^2}{\int_{\mathbb{R}} w^3\,dy} = 0.\end{aligned} \tag{3.7}$$

Combining (3.6), (3.7) and using (2.3) implies that $\hat\phi_1 = t_1\phi_1 + t_2\phi_2$ satisfies

$$\Delta\hat\phi_1 - \hat\phi_1 + 3\hat\phi_1 w^2 - 3\int w^3\hat\phi_1\,dy\,\frac{w^2}{\int w^3\,dy} = 0. \tag{3.8}$$

Multiplying (3.8) by w, integrating and using (1.3), we get

$$\int w^3\hat\phi_1\,dy = 0.$$

Thus the nonlocal term in (3.8) vanishes and we have

$$\Delta\hat\phi_1 - \hat\phi_1 + 3\hat\phi_1 w^2 = 0.$$

This implies $\hat\phi_1 = 0$ by Lemma 4.1 in [39] since it is an even function.

Thus, the nonlocal terms in (3.6), (3.7) vanish. Then for $\hat\phi_2 = t_2\phi_1 - t_1\phi_2$, we get

$$\Delta\hat\phi_2 - \hat\phi_2 + (3 - 2\beta(t_1^2 + t_2^2))\hat\phi_2 w^2 = 0$$

which implies $\hat\phi_2 = 0$ by Lemma 4.1 of [39] (see also in the Appendix). Going back to the original eigenfunctions, we have $\phi_1 = \phi_2 = 0$.

By the Closed Range Theorem it follows that the map L_ϵ is surjective. (The details are given for example in [38].) □

Next we complete the proof of Theorem 1. It is quite standard and based on the contraction mapping principle. We outline the argument for the system under consideration.

Proof of Theorem 1. The main existence result Theorem 1 can now be shown as follows:

We first compute $S_\epsilon[t_1\sqrt{v_\epsilon(0)}w\chi, t_2\sqrt{v_\epsilon(0)}w\chi]$. From the first equation of (1.2), we get

$$\epsilon^2 u_{1,xx} - u_1 + \frac{\mu_1 u_1^3 + \beta u_1 u_2^2}{v_\epsilon} = t_1\sqrt{v_\epsilon(0)}(w'' - w + w^3) + t_1\sqrt{v_\epsilon(0)}w^3\left(\frac{v_\epsilon(0)}{v_\epsilon(\epsilon y)} - 1\right) + O(\epsilon^3)$$

$$= 0 + t_1\sqrt{v_\epsilon(0)}w^3\left(-\frac{v_\epsilon''(0)\epsilon^2y^2}{2v_\epsilon(0)} + O(\epsilon^3|y|^3)\right) = O(\epsilon^2y^2w^3(y)).$$

Here we have used that $v_\epsilon(\epsilon y)$ is an even function and so $v_\epsilon'(0) = 0$ and the $O(\epsilon)$ term vanishes.

Since

$$S_\epsilon[t_1\sqrt{v_\epsilon(0)}w\chi + a_1, t_2\sqrt{v_\epsilon(0)}w\chi + a_2] = S_\epsilon[t_1\sqrt{v_\epsilon(0)}w\chi, t_2\sqrt{v_\epsilon(0)}w\chi] + L_\epsilon(a_1,a_2) + G(a_1,a_2),$$

where

$$\|S_\epsilon[t_1\sqrt{v_\epsilon(0)}w\chi, t_2\sqrt{v_\epsilon(0)}w\chi]\|_{(L^2(\Omega_\epsilon))^2} = O(\epsilon^2)$$

and

$$\|G(a_1,a_2)\|_{(L^2(\Omega_\epsilon))^2} = O((\|(a_1,a_2)\|_{(L^2(\Omega_\epsilon))^2})^2)$$

we can re-write

$$S_\epsilon[t_1\sqrt{v_\epsilon(0)}w\chi + a_1, t_2\sqrt{v_\epsilon(0)}w\chi + a_2] = 0$$

as

$$(a_1,a_2) = -L_\epsilon^{-1}S_\epsilon[t_1\sqrt{v_\epsilon(0)}w\chi, t_2\sqrt{v_\epsilon(0)}w\chi] - L_\epsilon^{-1}G(a_1,a_2).$$

In other words, we need to find a fixed point $(a_1,a_2) \in H_{2,ev}(\Omega_\epsilon)$ of the mapping

$$-L_\epsilon^{-1}S_\epsilon[t_1\sqrt{v_\epsilon(0)}w\chi, t_2\sqrt{v_\epsilon(0)}w\chi] - L_\epsilon^{-1}G(a_1,a_2) \ : \ H_{2,ev}(\Omega_\epsilon) \mapsto H_{2,ev}(\Omega_\epsilon).$$

The existence of this fixed point is guaranteed by the contraction mapping principle. The details follow closely the analysis for the Gierer–Meinhardt system, see for example Section 3 in [40] or Section 5 in [35]. The existence of Type 1 solutions follows. □

For the existence of Type 2 solutions, the proof is similar and is omitted. The nonlocal eigenvalue problem is given in (4.15) and (4.16) and no transformation of eigenfunctions is required. The result about the kernel of the nonlocal eigenvalue problem is given in Proposition 3. As for Type 1 solutions it has to be shown that the kernel of the adjoint operator is trivial. To prove this result we have to consider the same NLEP as in (3.8) but now applied to ϕ_1 instead of $\hat{\phi}_1$. The proof concludes in the same way as for Type 1 solutions.

In the next two sections we consider the stability or instability of these solutions.

4. Stability I: The eigenvalue problem and the large eigenvalues

Now we study the (linearized) stability of this even steady state. To this end, we first derive the linearized operator around the steady state $(u_1^\epsilon, u_2^\epsilon, v^\epsilon)$ given in Theorem 1.

We perturb the steady state as follows:

$$u_1 = u_1^\epsilon + \phi_1^\epsilon e^{\lambda t}, \quad u_2 = u_2^\epsilon + \phi_2^\epsilon e^{\lambda t}, \quad v = v_\epsilon + \psi^\epsilon e^{\lambda t}.$$

By linearization, we obtain the following eigenvalue problem (dropping superscripts and subscripts ϵ):

$$\begin{cases} \lambda_\epsilon\phi_1 = \epsilon^2\phi_{1,xx} - \phi_1 + \dfrac{3\mu_1u_1^2\phi_1 + \beta u_2^2\phi_1 + 2\beta u_1u_2\phi_2}{v} - \dfrac{\mu_1u_1^3 + \beta u_1u_2^2}{v^2}\psi, \\ \lambda_\epsilon\phi_2 = \epsilon^2\phi_{2,xx} - \phi_2 + \dfrac{3\mu_2u_2^2\phi_2 + \beta u_1^2\phi_2 + 2\beta u_1u_2\phi_1}{v} - \dfrac{\mu_2u_2^3 + \beta u_1^2u_2}{v^2}\psi, \\ \tau\lambda_\epsilon\psi = D\psi_{xx} - \psi + (3\mu_1u_1^2\phi_1 + \beta u_2^2\phi_1 + 2\beta u_1u_2\phi_2 + 3\mu_2u_2^2\phi_2 + \beta u_1^2\phi_2 + 2\beta u_1u_2\phi_1)\epsilon^{-1}, \end{cases} \tag{4.1}$$

where all components belong to the space $H_N^2(\Omega)$.

We now analyze the case $\lambda_\epsilon \to \lambda_0 \neq 0$ (large eigenvalues). We rescale $x = \epsilon y$, take the limit $\epsilon \to 0$ in (4.1), and note that ϕ_i converges locally in $H^2(\Omega_\epsilon)$. Then we get for the first two components, using the approximations of u_1 and u_2 given in Theorem 1:

$$\begin{cases} \lambda_\epsilon\phi_1 \sim \phi_{1,yy} - \phi_1 + \dfrac{3\mu_1u_1^2\phi_1 + \beta u_2^2\phi_1 + 2\beta u_1u_2\phi_2}{v(0)} - \dfrac{\mu_1u_1^3 + \beta u_1u_2^2}{v(0)^2}\psi(0), \\ \lambda_\epsilon\phi_2 \sim \phi_{2,yy} - \phi_2 + \dfrac{3\mu_2u_2^2\phi_2 + \beta u_1^2\phi_2 + 2\beta u_1u_2\phi_1}{v(0)} - \dfrac{\mu_2u_2^3 + \beta u_1^2u_2}{v(0)^2}\psi(0), \end{cases} \tag{4.2}$$

where $v(0)$ is given by (2.11).

Now we calculate the term $\psi(0)$. We consider the special case $\tau = 0$ using the Green's function G_D given in (2.7).

Remark 6. The case of small τ can be considered using a small perturbation of the case $\tau = 0$ as it can be shown that $|\lambda_\epsilon| \le C$ for all eigenvalues such that $\lambda_\epsilon > -c_0$ with some small $c_0 > 0$, for example using a characterization of the eigenvalues by quadratic forms [41]. Alternatively, one could consider the case of arbitrary τ using a more general Green's function.

From the third equation of (4.1) we get

$$\psi(0) \sim v(0)\left[[3\mu_1t_1^2 + \beta t_2^2 + 2\beta t_1t_2]\int_{\mathbb{R}} w^2\phi_1\,dy + [2\beta t_1t_2 + 3\mu_2t_2^2 + \beta t_1^2]\int_{\mathbb{R}} w^2\phi_2\,dy\right]G_D(0,0). \tag{4.3}$$

Recalling from (2.11) that

$$v(0) = \frac{1}{G_D(0,0)^2(t_1+t_2)^2\left(\int_{\mathbb{R}} w^3\right)^2} + O(\epsilon),$$

we get from (4.3)

$$\psi(0) \sim \frac{1}{G_D(0,0)(t_1+t_2)^2(\int_{\mathbb{R}} w^3 dy)^2} \times \left[[3\mu_1 t_1^2 + \beta t_2^2 + 2\beta t_1 t_2]\int_{\mathbb{R}} w^2\phi_1\, dy + [2\beta t_1 t_2 + 3\mu_2 t_2^2 + \beta t_1^2]\int_{\mathbb{R}} w^2\phi_2\, dy\right]. \tag{4.4}$$

Then (4.2) gives the following nonlocal eigenvalue problem (NLEP)

$$\Delta\phi_1 - \phi_1 + [(2\mu_1 t_1^2+1)\phi_1 + 2\beta t_1 t_2\phi_2]w^2 - \frac{t_1}{t_1+t_2}\left[(2\mu_1 t_1^2 + 1 + 2\beta t_1 t_2)\int_{\mathbb{R}} w^2\phi_1\, dy + (2\mu_2 t_2^2 + 1 + 2\beta t_1 t_2)\int_{\mathbb{R}} w^2\phi_2\, dy\right]\frac{w^3}{\int_{\mathbb{R}} w^3\, dy} = \lambda\phi_1, \tag{4.5}$$

$$\Delta\phi_2 - \phi_2 + [(2\mu_2 t_2^2+1)\phi_2 + 2\beta t_1 t_2\phi_1]w^2 - \frac{t_2}{t_1+t_2}\left[(2\mu_2 t_2^2 + 1 + 2\beta t_1 t_2)\int_{\mathbb{R}} w^2\phi_2\, dy + (2\mu_1 t_1^2 + 1 + 2\beta t_1 t_2)\int_{\mathbb{R}} w^2\phi_1\, dy\right]\frac{w^3}{\int_{\mathbb{R}} w^3\, dy} = \lambda\phi_2, \tag{4.6}$$

where $\phi_1, \phi_2 \in H^2(\mathbb{R})$.

We first diagonalize the local terms of the NLEP (4.5), (4.6). Written in vector form, the local terms are

$$\Delta\phi - \phi + \mathcal{B}\phi w^2, \tag{4.7}$$

where $\phi = (\phi_1, \phi_2)^T$ and

$$\mathcal{B} = \begin{pmatrix} 2\mu_1 t_1^2 + 1 & 2\beta t_1 t_2 \\ 2\beta t_1 t_2 & 2\mu_2 t_2^2 + 1 \end{pmatrix}. \tag{4.8}$$

Using (2.3), the eigenvalues of $\mathcal{B}$ are 3 and $3 - 2\beta(t_1^2 + t_2^2)$, with corresponding eigenvectors $(t_1, t_2)^T$ and $(-t_2, t_1)^T$, respectively.

Thus, setting

$$\hat{\phi}_1 = t_1\phi_1 + t_2\phi_2 \tag{4.9}$$

and

$$\hat{\phi}_2 = -t_2\phi_1 + t_1\phi_2, \tag{4.10}$$

the NLEP is transformed to

$$\Delta\hat{\phi}_1 - \hat{\phi}_1 + 3\hat{\phi}_1 w^2 - \left[3\int_{\mathbb{R}} w^2\hat{\phi}_1\, dy + \frac{t_1 - t_2}{t_1+t_2}(3 - 2\beta(t_1^2+t_2^2))\int_{\mathbb{R}} w^2\hat{\phi}_2\, dy\right]\frac{w^3}{\int w^3\, dy} = \lambda\hat{\phi}_1, \tag{4.11}$$

and

$$\Delta\hat{\phi}_2 - \hat{\phi}_2 + (3 - 2\beta(t_1^2+t_2^2))\hat{\phi}_2 w^2 = \lambda\hat{\phi}_2. \tag{4.12}$$

Note that the transformed NLEP has a special structure: the second equation is decoupled from the first equation and it is a local equation. Therefore it can be considered first. Only the first equation has a nonlocal term.

While the NLEP approach is rather standard, the derivation of the transformed NLEP and its special structure are specific to this problem. Careful adjustment of the general approach is required to extend the analysis to this case.

By Lemma 3.2 of [42] we have exact information about the eigenvalues of the NLEP

$$\Delta\phi - \phi + 3\phi w^2 - 3\int_{\mathbb{R}} w^2\phi\, dy\frac{w^3}{\int w^3\, dy} = \lambda\phi. \tag{4.13}$$

Using the identity $L_0 w^2 = 3w^2$, where $L_0\phi = \Delta\phi - \phi + 3\phi w^2$, it has been shown in [42] that the point spectrum for the non-selfadjoint problem (4.13) is real, and it can be determined exactly. For the principal eigenvalue we have

$$\lambda = 3\left(1 - \frac{\int_{\mathbb{R}} w^5\, dy}{\int_{\mathbb{R}} w^3\, dy}\right) = 3\left(1 - \frac{3}{2}\right) = -\frac{3}{2}$$

using $w(y) = \sqrt{2}\,\mathrm{sech}\, y$. Further, the continuous spectrum of (4.13) is $\lambda < -1$. The kernel of (4.13) equals span $\{w_y\}$.

In (4.12) we rewrite

$$3 - 2\beta(t_1^2+t_2^2) = 1 - 2g(\beta),$$

where $g(\beta) = \beta(t_1^2+t_2^2) - 1$. For stability, it will be crucial to determine the sign of $g(\beta)$. Using (2.3), (2.10), we compute

$$g(\beta) = (\beta - \mu_2)t_2^2 = \frac{(\beta-\mu_1)(\beta-\mu_2)}{\beta^2 - \mu_1\mu_2}.$$

Since $t_1^2 t_2^2 > 0$, from (2.10) we get $(\beta-\mu_1)(\beta-\mu_2) > 0$. Therefore $g(\beta)$ has the same sign as $\beta^2 - \mu_1\mu_2$. Therefore, $g(\beta) > 0$ if $\beta > \max(\mu_1, \mu_2)$ and $g(\beta) < 0$ if $\beta < \min(\mu_1, \mu_2)$.

Then for the kernel of the NLEP (4.5), (4.6) we have the following result:

Proposition 2. *Suppose that*

$$\beta > \max(\mu_1, \mu_2) \quad \text{or} \quad \beta < \min(\mu_1, \mu_2).$$

If $\lambda = 0$, we get for the NLEP (4.5), (4.6)

$$\phi_1 = t_1 \alpha w_y, \quad \phi_2 = t_2 \alpha w_y, \quad \textit{(with some real number } \alpha\textit{)}.$$

Proof. We apply Lemma 4.1 in [39] to the second equation of the transformed NLEP (4.11), (4.12) and get $\hat{\phi}_2 = 0$ since $g(\beta) \neq 0$. Then we apply Lemma 3.2 of [42] to the first equation and get $\hat{\phi}_1 = \alpha w_y$, where α is a real number.

Transforming back, for the kernel of the **original NLEP** (4.5), (4.6) we have

$$\phi_1 = t_1 \alpha w_y, \quad \phi_2 = t_2 \alpha w_y, \quad \text{(with some real number } \alpha\text{)}. \quad \square$$

We will show Theorems 3 and 4 in two parts. In this section, we will show that all the large eigenvalues of order $O(1)$ must have negative real part. In the next section, we will show that all the small eigenvalues of order $o(1)$ must have negative real part. Here is the first part of the proof.

Proof of Theorem 3 (*Part 1*)**.** We consider the eigenvalues of the transformed NLEP (4.11), (4.12). We first consider the case $\beta > \max(\mu_1, \mu_2)$. Then we have $g(\beta) > 0$. If $\mathrm{Re}(\lambda) \geq -c$ for some $c > 0$ small enough, and $\lambda \neq 0$, then by Lemma 4.1 (4) of [11] (see also in the Appendix) we have

$$\hat{\phi}_2 = 0.$$

Since $\hat{\phi}_2 = 0$, the first equation becomes

$$\Delta \hat{\phi}_1 - \hat{\phi}_1 + 3\hat{\phi}_1 w^2 - 3 \int w^2 \hat{\phi}_1 \, dy \, \frac{w^3}{\int w^3 \, dy} = \lambda \hat{\phi}_1.$$

Therefore, $\hat{\phi}_1$ satisfies (4.13). By Lemma 3.2 of [42] we have $\hat{\phi}_1 = 0$. Transforming back, this implies that $\phi_1 = \phi_2 = 0$, and there is no eigenvalue with $\mathrm{Re}(\lambda) \geq -c$ for some $c > 0$ small enough and $\lambda \neq 0$. The stability part of Theorem 3 follows.

If $\beta < \min(\mu_1, \mu_2)$, it follows that $g(\beta) < 0$ and we will show that the spike solutions are unstable.

In fact, by Lemma 4.1 (3) of [11] (see also in the Appendix), for (4.16) there is an eigenfunction $\hat{\phi}_2$ with $\lambda > 0$. Using this eigenfunction $\hat{\phi}_2$ we can compute $\hat{\phi}_1$ as follows:

Let

$$\mathcal{L}\hat{\phi}_1 = \Delta \hat{\phi}_1 - \hat{\phi}_1 + 3\hat{\phi}_1 w^2 - \frac{3w^3}{\int w^3 \, dy} \int w^2 \hat{\phi}_1 \, dy. \tag{4.14}$$

Note that the operator $\mathcal{L} - \lambda I : H^2(\mathbb{R}) \to L^2(\mathbb{R})$ is invertible by Lemma 3.2 of [42]. Then we compute

$$\hat{\phi}_1 = -(\mathcal{L} - \lambda I)^{-1} \frac{t_1 - t_2}{t_1 + t_2} (3 - 2\beta(t_1^2 + t_2^2)) \int w^2 \hat{\phi}_2 \, dy \frac{w^3}{\int w^3 \, dy}.$$

Transforming back, we get an eigenfunction (ϕ_1, ϕ_2) with eigenvalue $\lambda > 0$.

Arguing as in the proof of Theorem 1 of [43] (see also in the Appendix) the eigenvalue problem (4.5), (4.6) captures all converging sequences of eigenvalues λ_ϵ of (4.1) which converge to an eigenvalue λ with $\mathrm{Re}(\lambda) > -1$. On the other hand, for any eigenvalue λ of (4.5), (4.6) with $\mathrm{Re}(\lambda) > -1$ there is a converging sequence of eigenvalues λ_ϵ of (4.1) with λ as its limit. Therefore the eigenvalue problem (4.1) is stable concerning eigenvalues sequences λ_ϵ converging to a limit which is not zero. The proof of Theorem 3 (Part 1) is complete. $\square$

The proof of Theorem 4 follows the same strategy. For Type 2 spike solutions, using (4.2), the NLEP becomes

$$\Delta \phi_1 - \phi_1 + 3\phi_1 w^2 - \left[3 \int_\Omega w^2 \phi_1 \, dy + \frac{\beta}{\mu_1} \int_\Omega w^2 \phi_2 \, dy \right] \frac{w^3}{\int_\Omega w^3 \, dy} = \lambda \phi_1, \tag{4.15}$$

$$\Delta \phi_2 - \phi_2 + \frac{\beta}{\mu_1} \phi_2 w^2 = \lambda \phi_2, \tag{4.16}$$

where $\phi_1, \phi_2 \in H^2(\mathbb{R})$.

The NLEP has a special structure: Only the first equation is a NLEP. The second equation is a decoupled local equation. No transformation of the eigenfunctions is required.

First, we have the following result about the kernel of the NLEP (4.15), (4.16):

Proposition 3. *Suppose that $\frac{\beta}{\mu_1} \neq 1$. If $\lambda = 0$, we get for the NLEP (4.15), (4.16)$\phi_1 = \alpha w_y$, $\phi_2 = 0$, where α is a real number.*

Proof. We apply Lemma 4.1 in [39] to the second equation and get $\phi_2 = 0$. Then we apply Lemma 3.2 of [42] to the first equation and get $\phi_1 = \alpha w_y$, where α is a real number. $\square$

Proof of Theorem 4 (*Part 1*)**.** We consider the eigenvalues of the NLEP (4.15), (4.16). If $\mathrm{Re}(\lambda) \geq -c$ for some $c > 0$ small enough, and $\lambda \neq 0$, we get $\phi_2 = 0$, provided that $\frac{\beta}{\mu_1} < 1$, by using Lemma 4.1 (4) of [11]. Then we apply Lemma 3.2 of [42] to the first equation and get $\phi_1 = 0$. This implies **stability** of the eigenvalue problem (4.15), (4.16).

On the other hand, if $\frac{\beta}{\mu_1} > 1$ we can construct an unstable eigenfunction, first for ϕ_2, and then also for ϕ_1. In fact, by Lemma 4.1 (3) of [11], for (4.16) there is an eigenfunction ϕ_2 with $\lambda > 0$. Using this eigenfunction ϕ_2 we can compute ϕ_1 as follows:

Let $\mathcal{L}$ be the operator defined in (4.14) but now applied to ϕ_1 instead of $\hat{\phi}_1$. Recall that the operator $\mathcal{L}-\lambda I : H^2(\mathbb{R}) \to L^2(\mathbb{R})$ is invertible by Lemma 3.2 of [42]. Then we compute

$$\phi_1 = -(\mathcal{L}-\lambda I)^{-1}\frac{\beta}{\mu_1}\int w^2\phi_2\,dy\frac{w^3}{\int w^3\,dy}.$$

Thus (ϕ_1,ϕ_2) is an eigenfunction for eigenvalue $\lambda > 0$.

Again, using the argument [43], the eigenvalue problem (4.1) is stable concerning eigenvalue sequences λ_ϵ whose limit is not zero. The proof of Theorem 4 (Part 1) is complete. □

In the next section we will prove Theorem 3 (Part 2) and Theorem 4 (Part 2) by considering small eigenvalues λ_ϵ which converge to zero.

5. Stability II: The small eigenvalues

Now we study the small eigenvalues for (4.1), namely those with $\lambda_\epsilon \to 0$ as $\epsilon \to 0$. For simplicity, we set $\tau = 0$. Since $\tau\lambda_\epsilon \ll 1$ the results in this section are also valid for τ finite. The case of general $\tau > 0$ can be treated as in Section 7 of [33]. We will show that the small eigenvalues are of order $O(\epsilon^2)$.

The analysis of small eigenvalues has been performed for related problems. Here we need to carry out a transformation of the eigenvalue problem to adapt the general approach to this case.

Proof of Theorem 3 (*Part 2*)**.** For given $f \in L^2(\Omega)$, let $T[f]$ be the unique solution in $H^2_N(\Omega)$ of the problem

$$D\Delta(T[f]) - T[f] + \epsilon^{-1}f = 0. \tag{5.1}$$

We present the argument in detail for Type 1 solutions. We will explain the differences for Type 2 and Type 3 solutions in Remark 7.

By Theorem 1 we have for the spiky steady states

$$u_1^\epsilon = \hat{\imath}_1 w_\epsilon + O(\epsilon), \quad u_2^\epsilon = \hat{\imath}_2 w_\epsilon + O(\epsilon),$$

$$v_\epsilon = T[\mu_1(u_1^\epsilon)^3 + \beta u_1^\epsilon(u_2^\epsilon)^2 + \mu_2(u_2^\epsilon)^3 + \beta(u_1^\epsilon)^2u_2^\epsilon], \tag{5.2}$$

where

$$\hat{t}_i = \sqrt{v_\epsilon(0)}t_i. \tag{5.3}$$

After rescaling $x = \epsilon y$ for the first two components, the eigenvalue problem (4.1) becomes

$$\begin{aligned}
\lambda_\epsilon\phi_1 &= \phi_{1,yy} - \phi_1 + \frac{3\mu_1(u_1^\epsilon)^2\phi_1 + \beta(u_2^\epsilon)^2\phi_1 + 2\beta u_1^\epsilon u_2^\epsilon\phi_2}{v_\epsilon} - \frac{\mu_1(u_1^\epsilon)^3 + \beta u_1^\epsilon(u_2^\epsilon)^2}{v_\epsilon^2}\psi,\\
\lambda_\epsilon\phi_2 &= \phi_{2,yy} - \phi_2 + \frac{3\mu_2(u_2^\epsilon)^2\phi_2 + \beta(u_1^\epsilon)^2\phi_2 + 2\beta u_1^\epsilon u_2^\epsilon\phi_1}{v_\epsilon} - \frac{\mu_2(u_2^\epsilon)^3 + \beta(u_1^\epsilon)^2u_2^\epsilon}{v_\epsilon^2}\psi,\\
\tau\lambda_\epsilon\psi &= D\psi_{xx} - \psi + \left[3\mu_1(u_1^\epsilon)^2\phi_1 + \beta(u_2^\epsilon)^2\phi_1 + 2\beta u_1^\epsilon u_2^\epsilon\phi_2 + 3\mu_2(u_2^\epsilon)^2\phi_2 + \beta(u_1^\epsilon)^2\phi_2 + 2\beta u_1^\epsilon u_2^\epsilon\phi_1\right]\epsilon^{-1},
\end{aligned} \tag{5.4}$$

where the unknown functions ϕ_1, ϕ_2 are in $H^2_N(\Omega_\epsilon)$ and ψ is in $H^2_N(\Omega)$.

Let us define

$$\tilde{u}_{\epsilon,j}(\epsilon y) = \chi(\epsilon y)u_j^\epsilon(\epsilon y), \quad j = 1, 2, \tag{5.5}$$

where χ is the smooth, even cut-off function defined in (3.1). Then

$$\tilde{u}_{\epsilon,j}(x) = u_j^\epsilon(x) + \text{e.s.t.}, \quad j = 1, 2, \tag{5.6}$$

where e.s.t. denotes an exponentially small term in $H^2_N(\Omega_\epsilon)$. We note that $\tilde{u}_{\epsilon,j}$, $j = 1, 2$ are even functions.

Next we transform the eigenfunctions as in (4.9), (4.10):

$$\hat{\phi}_1 = t_1\phi_1 + t_2\phi_2,$$

$$\hat{\phi}_2 = -t_2\phi_1 + t_1\phi_2.$$

The transformed eigenvalue problem becomes in leading order

$$\begin{aligned}
\lambda_\epsilon\hat{\phi}_1 &= \hat{\phi}_{1,yy} - \hat{\phi}_1 + 3w^2\chi^2\hat{\phi}_1\frac{v_\epsilon(0)}{v_\epsilon}(1+O(\epsilon)) - (t_1^2+t_2^2)w^3\chi^3\frac{(v_\epsilon(0))^{3/2}\hat{\psi}}{v_\epsilon^2}(1+O(\epsilon)),\\
\lambda_\epsilon\hat{\phi}_2 &= \hat{\phi}_{2,yy} - \hat{\phi}_2 + (3-2\beta(t_1^2+t_2^2))w^2\chi^2\hat{\phi}_2\frac{v_\epsilon(0)}{v_\epsilon}(1+O(\epsilon)),\\
\tau\lambda_\epsilon\hat{\psi} &= D\hat{\psi}_{xx} - \hat{\psi} + \left[3w^2\chi^2\hat{\phi}_1 + \tfrac{t_1-t_2}{t_1+t_2}(3-2\beta(t_1^2+t_2^2))w^2\chi^2\hat{\phi}_2\right]v_\epsilon(0)\epsilon^{-1}(1+O(\epsilon)),
\end{aligned} \tag{5.7}$$

where all unknown functions $\hat{\phi}_1$, $\hat{\phi}_2$, $\hat{\psi}$ are in $H^2_N(\Omega)$.

Next we define the approximate kernel and co-kernel for the transformed eigenvalue problem (5.7)

$$\mathcal{K}_\epsilon := \text{span}\left\{\left(t_1\frac{d}{dy}\tilde{u}_{\epsilon,1}(\epsilon y) + t_2\frac{d}{dy}\tilde{u}_{\epsilon,2}(\epsilon y), 0\right)\right\} \subset (H^2_N(\Omega_\epsilon))^2,$$

$$C_\epsilon := \text{span}\left\{\left(t_1\frac{d}{dy}\tilde{u}_{\epsilon,1}(\epsilon y)+t_2\frac{d}{dy}\tilde{u}_{\epsilon,2}(\epsilon y),0\right)\right\}\subset (L^2(\Omega_\epsilon))^2,$$

where $\Omega_\epsilon=\left(-\frac{L}{\epsilon},\frac{L}{\epsilon}\right)$.

Note that, by Theorem 1, $\tilde{u}_{\epsilon,j}$ satisfies

$$\Delta_y\tilde{u}_{\epsilon,j}-\tilde{u}_{\epsilon,j}+\frac{\mu_j\tilde{u}_{\epsilon,j}^3+\beta\tilde{u}_{\epsilon,j}\tilde{u}_{\epsilon,3-j}^2}{v_\epsilon}+\text{e.s.t}=0,\quad j=1,2.$$

Thus $\tilde{u}'_{\epsilon,j}:=\frac{d\tilde{u}_{\epsilon,j}}{dy}$, $v'_\epsilon:=\epsilon\frac{dv_\epsilon(x)}{dx}$ satisfies

$$\Delta_{yy}\tilde{u}'_{\epsilon,j}-\tilde{u}'_{\epsilon,j}+\frac{3\mu_1\tilde{u}_{\epsilon,j}^2+\beta\tilde{u}_{\epsilon,3-j}^2}{v_\epsilon}\tilde{u}'_{\epsilon,j}+\frac{2\beta\tilde{u}_{\epsilon,j}\tilde{u}_{\epsilon,3-j}}{v_\epsilon}\tilde{u}'_{\epsilon,3-j}-\frac{\mu_j\tilde{u}_{\epsilon,j}^3+\beta\tilde{u}_{\epsilon,j}\tilde{u}_{\epsilon,3-j}^2}{(v_\epsilon)^2}v'_\epsilon+\text{e.s.t}=0. \tag{5.8}$$

This implies

$$\begin{aligned}&(t_1\tilde{u}'_{\epsilon,1}+t_2\tilde{u}'_{\epsilon,2})_{yy}-(t_1\tilde{u}'_{\epsilon,1}+t_2\tilde{u}'_{\epsilon,2})+\frac{3w^2\chi^2v_\epsilon(0)}{v_\epsilon}(t_1\tilde{u}'_{\epsilon,1}+t_2\tilde{u}'_{\epsilon,2})\\&\quad-\frac{(t_1^2+t_2^2)\chi^3w^3(v_\epsilon(0))^{3/2}}{(v_\epsilon)^2}v'_\epsilon+O(\epsilon)=0.\end{aligned} \tag{5.9}$$

Let us now decompose $\hat{\phi}_\epsilon=(\hat{\phi}_{\epsilon,1},\hat{\phi}_{\epsilon,2})$, where

$$\hat{\phi}_{\epsilon,1}=a^\epsilon(t_1\tilde{u}'_{\epsilon,1}+t_2\tilde{u}'_{\epsilon,2})+\phi_\epsilon^\perp, \tag{5.10}$$

with complex numbers a^ϵ. Here the factor ϵ is for scaling purposes, to achieve that a^ϵ is of order $O(1)$, and

$$(\phi_\epsilon^\perp,0)\in\mathcal{K}_\epsilon^\perp,$$

where orthogonality is taken with respect to the scalar product of the product space $(L^2(\Omega_\epsilon))^2$. We will show that

$$\|\phi_\epsilon^\perp\|_{H^2(\Omega_\epsilon)}=O(\epsilon^2),\quad \|\hat{\phi}_{\epsilon,2}\|_{H^2(\Omega_\epsilon)}=O(\epsilon^2),$$

and so $\phi_\epsilon^\perp$ and $\hat{\phi}_{\epsilon,2}$ will not play a leading role in our results.

Suppose that $\|\phi_\epsilon\|_{H^2(\Omega_\epsilon)}=1$. Then $|a^\epsilon|\le C$.

Similarly, we decompose

$$\psi_\epsilon=a^\epsilon\psi_{\epsilon,1}+\psi_\epsilon^\perp, \tag{5.11}$$

where $\psi_{\epsilon,1}$ satisfies

$$\psi_{\epsilon,1}=T[3w^2\chi^2(t_1\tilde{u}'_{\epsilon,1}+t_2\tilde{u}'_{\epsilon,2})]v_\epsilon(0)(1+O(\epsilon)) \tag{5.12}$$

and $\psi_\epsilon^\perp$ is given by

$$\psi_\epsilon^\perp=T[3w^2\chi^2\phi_\epsilon^\perp+\frac{t_1-t_2}{t_1+t_2}(3-2\beta(t_1^2+t_2^2))w^2\chi^2\hat{\phi}_2]v_\epsilon(0)(1+O(\epsilon)). \tag{5.13}$$

By the second equation of (5.7) we get

$$\hat{\phi}_{\epsilon,2,yy}-(1+\lambda_\epsilon)\hat{\phi}_{\epsilon,2}+(3-2\beta(t_1^2+t_2^2))w^2\chi^2\hat{\phi}_{\epsilon,2}\frac{v_\epsilon(0)}{v_\epsilon(\epsilon y)}(1+O(\epsilon))=0.$$

Since

$$\frac{v_\epsilon(0)}{v_\epsilon(\epsilon y)}=1-\frac{1}{2(v_\epsilon(0))}v''_\epsilon(0)\epsilon^2y^2+O(\epsilon^3|y|^3)=1+O(\epsilon^2y^2) \tag{5.14}$$

we get $\|\hat{\phi}_{\epsilon,2}\|_{H^2(\Omega_\epsilon)}=O(\epsilon^2)$. Here we have used that $v_\epsilon(\epsilon y)$ is an even function and so $v'_\epsilon(0)=0$ and the $O(\epsilon)$ term vanishes.

Substituting the decomposition of $\hat{\phi}_{\epsilon,1}$ and ψ_ϵ as well as $\hat{\phi}_{\epsilon,2}$ into the first part of (5.7) we have

$$\begin{aligned}&\epsilon\left(a^\epsilon(t_1^2+t_2^2)w^3\chi^3\frac{v_\epsilon(0)^{3/2}}{v_\epsilon^2}v'_\epsilon-a^\epsilon(t_1^2+t_2^2)\frac{w^3\chi^3(v_\epsilon(0))^{3/2}}{v_\epsilon^2}\psi_{\epsilon,1}\right)\\&\quad+\Delta\phi_\epsilon^\perp-\phi_\epsilon^\perp+3w^2\chi^2\frac{v_\epsilon(0)}{v_\epsilon}\phi_\epsilon^\perp-\frac{(t_1^2+t_2^2)w^3\chi^3(v_\epsilon(0))^{3/2}}{v_\epsilon^2}\psi_\epsilon^\perp-\lambda_\epsilon\phi_\epsilon^\perp+\text{e.s.t}\\&=\lambda_\epsilon a^\epsilon(t_1^2+t_2^2)\sqrt{v_\epsilon(0)}w'(1+o(1)),\end{aligned} \tag{5.15}$$

since $t_1\tilde{u}'_{\epsilon,1}+t_2\tilde{u}'_{\epsilon,2}$ satisfies (5.9) and $t_1\tilde{u}'_{\epsilon,1}+t_2\tilde{u}'_{\epsilon,2}\sim(t_1^2+t_2^2)\sqrt{v_\epsilon(0)}w'$.

Using $\|\psi_\epsilon^\perp\|=O(\|\phi_\epsilon\|^\perp)+O(\epsilon^2)$, we derive $\|\phi_\epsilon^\perp\|=O(\epsilon^2)$ and $\|\psi_\epsilon^\perp\|=O(\epsilon^2)$ since the operator $\mathcal{L}-\lambda I$ with $\mathcal{L}$ defined in (4.14) is invertible by Lemma 3.2 of [42].

Multiplying both sides of (5.15) by w' and integrating, the l.h.s and the r.h.s of (5.15) become

$$\text{l.h.s.}=a^\epsilon(t_1^2+t_2^2)\sqrt{v_\epsilon(0)}\int_{\mathbb{R}}w^3\chi^3\frac{v_\epsilon(0)}{v_\epsilon^2}(v'_\epsilon-\psi_{\epsilon,1})w'\,dy+O(\epsilon^3) \tag{5.16}$$

and

$$\text{r.h.s.}=\lambda_\epsilon a^\epsilon(t_1^2+t_2^2)\sqrt{v_\epsilon(0)}\int_{\mathbb{R}}(w'(y))^2\,dy(1+o(1)), \tag{5.17}$$

respectively.

Note that the integrals resulting from the second line of (5.15) are in leading order a product of an even function of order $O(\epsilon^2)$ and an odd function. Therefore, for the integrals the terms of $O(\epsilon^2)$ vanish and they can estimated by $O(\epsilon^3)$.

Using the Green's function representations of v_ϵ and ψ_ϵ we compute using (2.7)

$$\begin{aligned}
&v_\epsilon'(\epsilon y) - \psi_{\epsilon,1}(\epsilon y)\\
&\quad = -(t_1+t_2)(v_\epsilon(0))^{3/2}\epsilon \int_{\mathbb{R}} \Big(\nabla_1 H_D(\epsilon y, \epsilon z) w^3(z) - H_D(\epsilon y, \epsilon z)\frac{d}{dz} w^3(z)\Big)\, dz + O(\epsilon^2)\\
&\quad = -(t_1+t_2)(v_\epsilon(0))^{3/2}\epsilon \int_{\mathbb{R}} (\nabla_1 H_D(\epsilon y, \epsilon z) + \nabla_2 H_D(\epsilon y, \epsilon z)) w^3(z)\, dz + O(\epsilon^2)\\
&\quad = -(t_1+t_2)(v_\epsilon(0))^{3/2}\epsilon (\nabla_1 H_D(\epsilon y, 0) + \nabla_2 H_D(\epsilon y, 0)) \int_{\mathbb{R}} w^3(z)\, dz + O(\epsilon^2),
\end{aligned}$$

where $\nabla_1 H_D(P,Q) = \frac{\partial}{\partial P} H_D(P,Q)$ and $\nabla_2 H_D(P,Q) = \frac{\partial}{\partial Q} H_D(P,Q)$.

We have used that the contribution from K_D vanishes. This can be seen as follows: since $K_D(x,y) = K_D(|x-y|)$ we compute

$$\begin{aligned}
&\int_{\mathbb{R}} \frac{\partial}{\partial y} K_D(|\epsilon y - \epsilon z|) w^3(z)\, dz = -\int_{\mathbb{R}} \Big(\frac{\partial}{\partial z} K_D(|\epsilon y - \epsilon z|)\Big) w^3(z)\, dz\\
&\quad = \int_{\mathbb{R}} K_D(|\epsilon y - \epsilon z|) \frac{d}{dz} w^3(z)\, dz.
\end{aligned}$$

Compare Section 7 of [33].

For (5.16), we get

$$\begin{aligned}
&\text{l.h.s.} =\\
&\quad = -\epsilon a^\epsilon (t_1^2+t_2^2)\sqrt{v_\epsilon(0)} \int_{\mathbb{R}} (t_1+t_2)\sqrt{v_\epsilon(0)} w'(y) w^3(y) (\nabla_1 H_D(\epsilon y, 0) + \nabla_2 H_D(\epsilon y, 0))\, dy\\
&\qquad \times \int_{\mathbb{R}} w^3(z)\, dz + O(\epsilon^3)\\
&\quad = -\epsilon^2 a^\epsilon (t_1^2+t_2^2)(t_1+t_2) v_\epsilon(0) \int_{\mathbb{R}} w'(y) w^3(y) y\, dy ((\nabla_1)^2 H_D(0,0) + \nabla_1\nabla_2 H_D(0,0))\\
&\qquad \times \int_{\mathbb{R}} w^3(z) dz + O(\epsilon^3)\\
&\quad = \epsilon^2 a^\epsilon (t_1^2+t_2^2)(t_1+t_2) v_\epsilon(0) \Big(\frac{1}{4}\int_{\mathbb{R}} w^4(y)\, dy\Big)\Big(\int_{\mathbb{R}} w^3(z)\, dz\Big)\\
&\qquad \times ((\nabla_1)^2 H_D(0,0) + \nabla_1\nabla_2 H_D(0,0)) + O(\epsilon^3)\\
&\quad = \epsilon^2 a^\epsilon (t_1^2+t_2^2)(t_1+t_2) v_\epsilon(0) \Big(\frac{1}{4}\int_{\mathbb{R}} w^4\, dy\Big)\Big(\int_{\mathbb{R}} w^3\, dz\Big)\\
&\qquad \times \Big(\nabla_P^2 H_D(P,Q)|_{P=Q=0} + \nabla_P\nabla_Q H_D(P,Q)|_{P=Q=0}\Big) + O(\epsilon^3)\\
&\quad = \epsilon^2 a^\epsilon (t_1^2+t_2^2)(t_1+t_2) v_\epsilon(0) \Big(\frac{1}{8}\int_{\mathbb{R}} w^4\, dy\Big)\Big(\int_{\mathbb{R}} w^3\, dz\Big) \nabla_P^2 H_D(P,P)|_{P=0} + O(\epsilon^3).
\end{aligned} \tag{5.18}$$

Combining (5.17) and (5.18), the small eigenvalues λ_ϵ satisfy

$$\lambda_\epsilon \sim \epsilon^2 (t_1+t_2)\sqrt{v_\epsilon(0)} \Big(\frac{1}{8}\int_{\mathbb{R}} w^4\, dy\Big)\Big(\int_{\mathbb{R}} w^3\, dz\Big) \frac{1}{\int_{\mathbb{R}} (w')^2\, dy} \nabla_P^2 H_D(P,P)|_{P=0}. \tag{5.19}$$

Using (2.11), we get

$$\lambda_\epsilon \sim \epsilon^2 \frac{\int_{\mathbb{R}} w^4\, dy}{8\int_{\mathbb{R}} (w')^2\, dy} \frac{\nabla_P^2 H_D(P,P)|_{P=0}}{G_D(0,0)}. \tag{5.20}$$

Since $G_D(0,0) > 0$ and $\nabla_P^2 H_D(P,P) < 0$ it follows that $\lambda_\epsilon < 0$. These inequalities can be derived from (2.7) as follows:

$$G_D(P,P) = \frac{\theta}{\sinh(2\theta L)} \cosh\theta(L+P)\cosh\theta(L-P),$$

$$G_D(0,0) = \frac{\theta}{\sinh(2\theta L)} \cosh^2(\theta L) = \frac{\theta}{2}\coth(\theta L) > 0,$$

$$\nabla_P^2 H_D(P,P)|_{P=0} = -\nabla_P^2 G_D(P,P)|_{P=0} = -\frac{2\theta^3}{\sinh(2\theta L)} \cosh^2(2\theta P)|_{P=0} = -\frac{2\theta^3}{\sinh(2\theta L)} < 0.$$

Now the proof of Theorem 3 is complete. □

Remark 7. For Type 2 and Type 3 spikes we can make similar computations for the small eigenvalues. We do not have to make the transformation of the eigenfunctions and we use the same Green's function G_D. We get

$$\lambda_\epsilon \sim \epsilon^2 t_1 \sqrt{v_\epsilon(0)} \Big(\frac{1}{8}\int_{\mathbb{R}} w^4\, dy\Big)\Big(\int_{\mathbb{R}} w^3(z)\, dz\Big) \frac{1}{\int_{\mathbb{R}} (w')^2\, dy} \nabla_P^2 H_D(P,P)|_{P=0}. \tag{5.21}$$

Using (2.15), we get

$$\lambda_\epsilon \sim \epsilon^2 \frac{\int_{\mathbb{R}} w^4\, dy}{8\int_{\mathbb{R}} (w')^2\, dy} \frac{\nabla_P^2 H_D(P,P)|_{P=0}}{G_D(0,0)}. \tag{5.22}$$

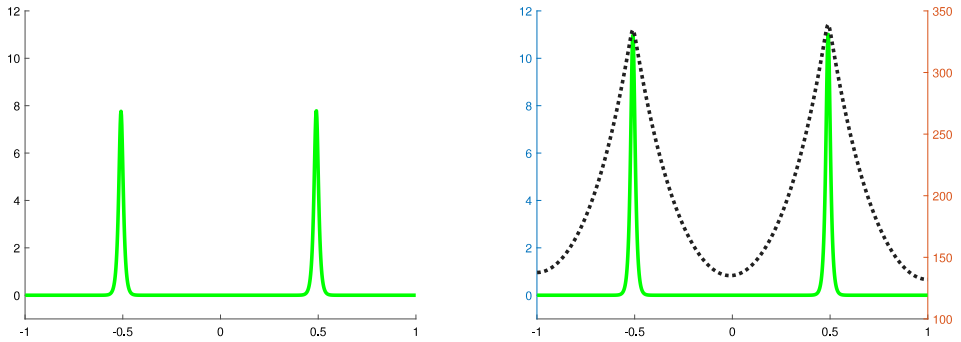

Fig. 5. Type 1 solution ($u_1 > 0, u_2 > 0$), color green, 2 spikes, $\epsilon^2 = 0.0001$, $D = 0.1$, $\mu_1 = 1$, $\mu_2 = 3$, $\beta = 5$.

We can see that the small eigenvalues for the Type 2 and Type 3 solutions are the same as for the Type 1 solutions. Since $G_D(0,0) > 0$ and $\nabla_P^2 H_D(P,P) < 0$ it follows that $\lambda_\epsilon < 0$.

Theorem 4 follows along the same lines as Theorem 3. □

In the next section we present some numerical computations of solutions which are beyond the scope of our analytical results.

6. Numerical simulations

We present some numerical simulations of solutions which are more general than the main results in Section 1.

We compute (1.1) with initial conditions $u_i(x,0) = 0.4 + 0.2\cos(100 * \pi x)$, $v(x,0) = 1.8 + 0.2\cos(100 * \pi x)$. The motivation for these initial conditions is to have spatial oscillations on a small scale.

Depending on the size of the inhibitor diffusivity D, single or multiple spikes will be triggered by these initial conditions in the first stage of the numerical simulation. After the shape of the spikes has formed, their amplitudes will converge quickly and their location will converge slowly to the final steady state. For (1.1) we use parameters $\epsilon^2 = 0.0001$, $\tau = 0.1$, and $D = 0.1$, $D = 0.01$ or $D = 0.001$.

The choice of constants for the numerical simulations has been motivated by the analysis. In the analysis we assumed that ϵ is "small enough". In the numerical simulation we chose $\epsilon^2 = 0.001$ so that the spike width of order $\sqrt{\epsilon} \sim \sqrt{0.001} \approx 0.032$ is small compared to the domain size. We also chose D larger than ϵ by at least factor 10, otherwise there might not be any patterns at all due to the Turing instability condition.

For μ_1, μ_2, β we use different settings so that we can get Type 1, Type 2 and Type 3 solutions. From the main results, what matters is the relative size of these parameters. The solutions we computed numerically as large time limits are all locally stable according to Theorems 3 and 4, respectively.

The analysis in this paper focused on single spike solutions and these are achieved when D is relatively large. For smaller values of D we can get more and more spikes.

We refer the discussion in the next section for further comments about the stability thresholds for D depending on the number of spikes (Section 7, item 3).

We solved the system using the commercial software COMSOL Multiphyisics 3.5a. For the time stepping we chose the relative tolerance 10^{-3}, absolute tolerance 10^{-4} and we solved up to time $5 \cdot 10^4$–10^6. We used the linear system solver Direct (UMFPACK) in every time step with pivot threshold 0.1, memory allocation factor 0.7 and automatic matrix symmetry. The time stepping method was backward differentiation formula (BDF) with timestep 10^{-2}, initial time step 10^{-3} and maximum time step 10^{-1}. The maximum BDF order was 5 and the minimum BDF order was 1, singular mass matrix was allowed. The constraint handling method was elimination, the null-space function was automatic, assembly block size was 10^3, solution form was set to automatic. We set the mesh size to $2 \cdot 10^{-3}$.

After time $5 \cdot 10^4$–10^6 the time-dependent solution was well converged to the steady state in all cases. We did not see any visible change when the simulation was continued. We expect an error of the order $e^{-\lambda_\epsilon t}$ due to the slow convergence of the positions of the spikes coming from small eigenvalues of order $o(1)$, see [30]. Recall that for the single spike solutions considered here the small eigenvalues λ_ϵ are given by (5.19) and (5.21), respectively. We computed for longer time 10^6 in the case of multiple spikes solutions since convergence was slower and for shorter time $5 \cdot 10^4$ in the case of single spikes.

Further, there is an error of order h^α with $\alpha \geq 1$ due to spatial discretization for step size h. We chose step size $h = 2 \cdot 10^{-3}$ to achieve a small enough spatial error.

The figures show the numerically obtained long-term limit of the three components u_1, u_2, v, i.e. the state at $5 \cdot 10^4$–10^6.

We compute all three types of spiky pattern solutions: Solutions of Type 1 which have spikes for u_1 and spikes for u_2. Solutions of Type 2 which have spikes for u_1 but $u_2 = 0$. Solutions of Type 3 which have spikes for u_2 but $u_1 = 0$. Finally, we have computed spike solutions which are a combination of Type 2 and Type 3 in different parts of the spatial domain.

The first subfigure always shows u_1 (solid line), the second subfigure shows u_2 (left axis, solid line) and v (right axis, dotted line) (see Figs. 5–12).

7. Discussion and outlook

In this final section, we discuss some possible generalizations, extensions and related topics.

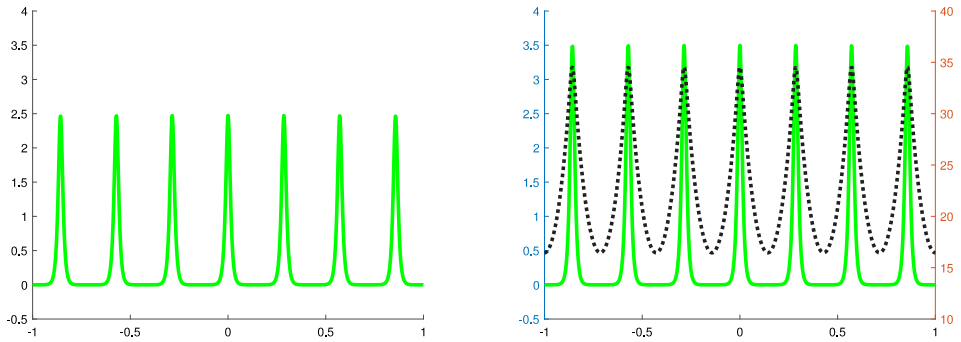

Fig. 6. Type 1 solution ($u_1 > 0$, $u_2 > 0$), color green, 7 spikes, $\epsilon^2 = 0.0001$, $D = 0.01$, $\mu_1 = 1$, $\mu_2 = 3$, $\beta = 5$.

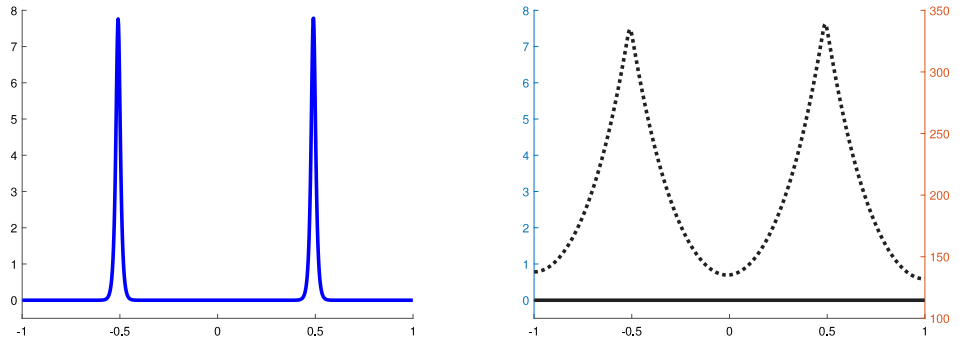

Fig. 7. Type 2 solution ($u_1 > 0$, $u_2 = 0$), color blue, 2 spikes, $\epsilon^2 = 0.0001$, $D = 0.1$, $\mu_1 = 1$, $\mu_2 = 3$, $\beta = 0.5$.

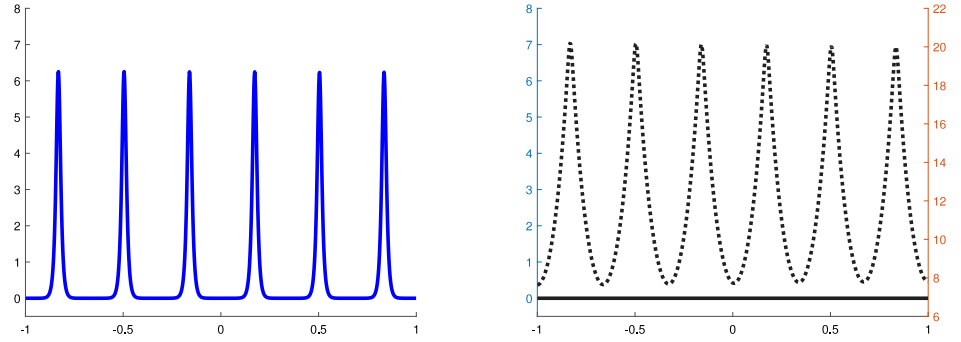

Fig. 8. Type 2 solution ($u_1 > 0$, $u_2 = 0$), color blue, 6 spikes, $\epsilon^2 = 0.0001$, $D = 0.01$, $\mu_1 = 1$, $\mu_2 = 3$, $\beta = 0.5$.

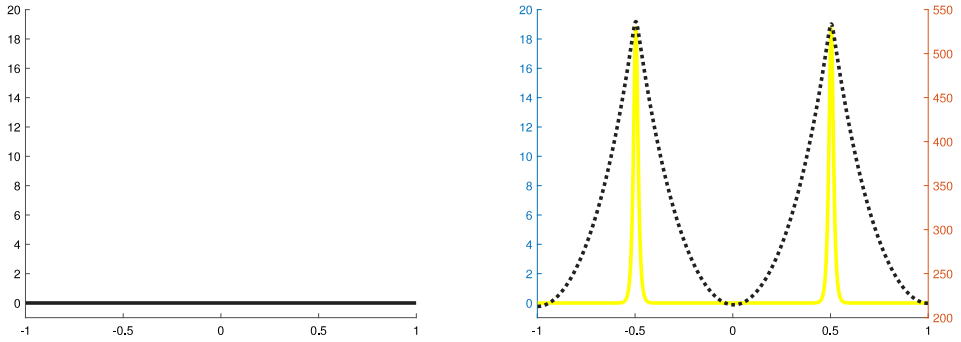

Fig. 9. Type 3 solution ($u_1 = 0$, $u_2 > 0$),color yellow, 2 spikes, $\epsilon^2 = 0.0001$, $D = 0.1$, $\mu_1 = 1$, $\mu_2 = 3$, $\beta = 2$.

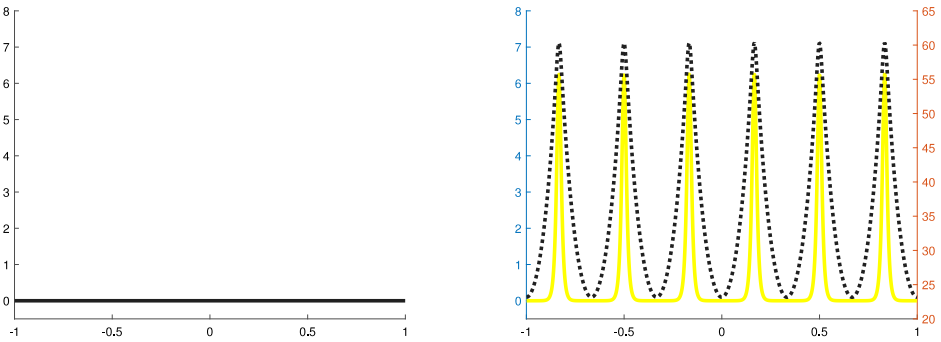

Fig. 10. Type 3 solution ($u_1 = 0$, $u_2 > 0$), color yellow, 6 spikes, $\epsilon^2 = 0.0001$, $D = 0.01$, $\mu_1 = 1$, $\mu_2 = 3$, $\beta = 2$.

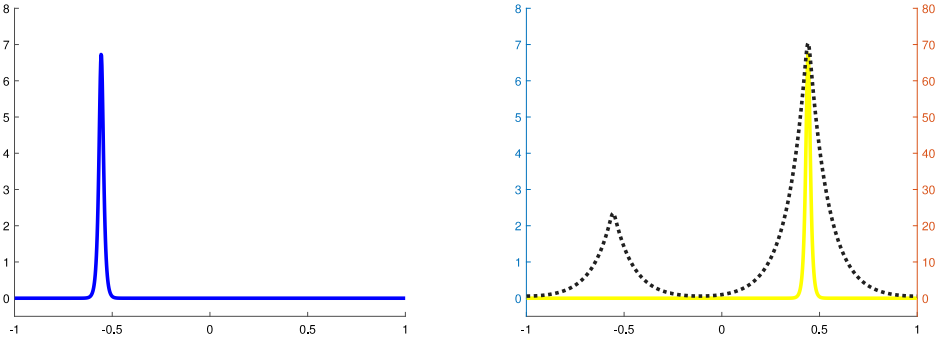

Fig. 11. Type 2/3 solution combined, colors blue/yellow, 1/1 spikes in different locations, $\epsilon^2 = 0.0001$, $D = 0.01$, $\mu_1 = 1$, $\mu_2 = 3$, $\beta = 0.5$.

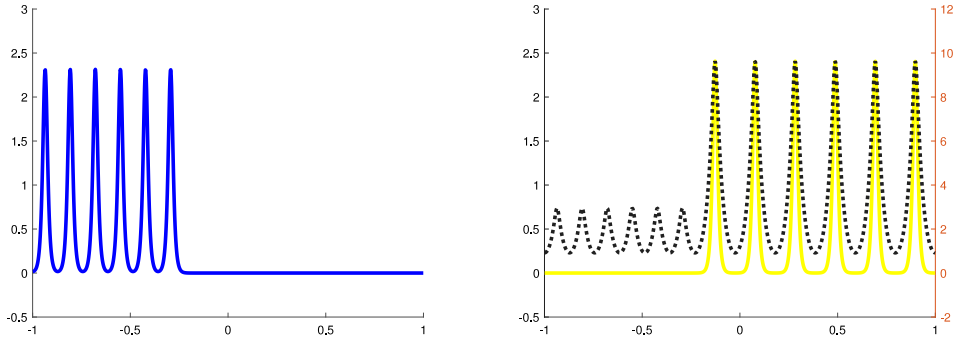

Fig. 12. Type 2/3 solution combined, colors blue/yellow, 6/6 spikes in different locations, $\epsilon^2 = 0.0001$, $D = 0.001$, $\mu_1 = 1$, $\mu_2 = 3$, $\beta = 0.5$.

1. It seems that the results and proofs can be generalized to the following system with general powers of the activator interaction rates:

$$\begin{cases} u_{1,t} = \epsilon^2 u_{1,xx} - u_1 + \dfrac{\mu_1 u_1^{p_1} + \beta u_1^{p_2} u_2^{p_3}}{v^q}, \quad u_{2,t} = \epsilon^2 u_{2,xx} - u_2 + \dfrac{\mu_2 u_2^{p_1} + \beta u_1^{p_2} u_2^{p_3}}{v^q}, \\ \tau v_t = D v_{xx} - v + \dfrac{\mu_1 u_1^{r_1} + \beta u_1^{r_2} u_2^{r_3} + \mu_2 u_2^{r_1} + \beta u_1^{r_2} u_2^{r_3}}{v^s}, \end{cases}$$

where $p_1 = p_2 + p_3$ and all p_i are positive, $r_1 = r_2 + r_3$ and all r_i are positive. It may be possible to relax some of these conditions but then the analysis will be more technical and the results will be less explicit. Further, it is assumed that

$$q > 0, \quad s \geq 0, \quad \frac{q r_1}{p_1 - 1} > s + 1$$

which is a generalization of the condition for the standard Gierer–Meinhardt system.

2. Motivated by the results in [31] for the standard Gierer–Meinhardt system, we expect Hopf bifurcation for sufficiently large τ, resulting in oscillating spikes. Our analysis covered only the case $\tau = 0$ for which oscillations are not possible. We explored this issue numerically in the some cases and found the following amplitude oscillations of the spikes or convergence of the solution to zero.

In the simulations we computed (1.1) with $D = 1$, $\epsilon^2 = 0.0001$, and initial conditions $u_i(x, 0) = 0.4 + 0.2\cos(\pi x)$, $v(x, 0) = 1.8 + 0.2\cos(\pi x)$. For small values of τ we observed a single spike steady state. We increased the value of τ in steps of 0.1 until the solution became unstable.

In particular, for $\mu_1 = \mu_2 = 0$, $\beta = 5$, and $\tau = 0.5$, we observed a single spike for u_1 and u_2 with simultaneous amplitude oscillations. For (1.1) with $\mu_1 = 1$, $\mu_2 = 3$, $\beta = 0$, and $\tau = 1.4$, we observed a single spike for u_2 only with amplitude oscillations, with u_1 converging to zero for large

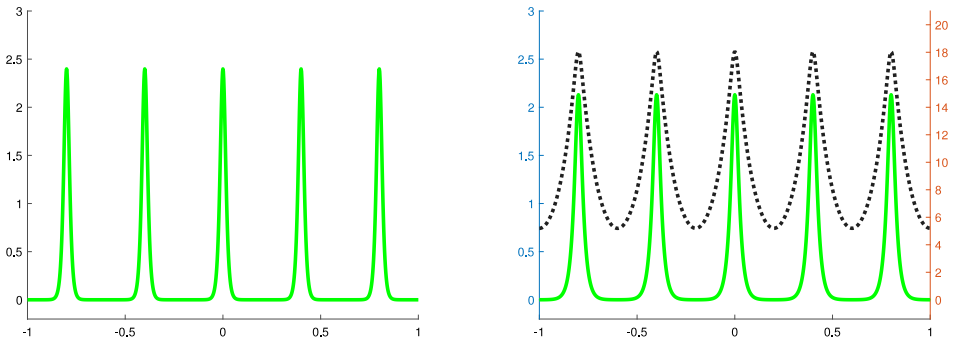

Fig. 13. Type 1 solution, color green, 5 spikes, $\epsilon_1^2 = 0.0001$, $\epsilon_2^2 = 0.0004$, $D = 0.01$, $\mu_1 = 1$, $\mu_2 = 3$, $\beta = 5$.

time. For $\mu_1 = 1$, $\mu_2 = 3$, $\beta = 5$, and $\tau = 0.6$, we observed that u_1 and u_2 both converge to zero for large time. It will be interesting to study this topic analytically and numerically in a systematic way.

3. The analysis can be extended from single spikes to multiple spikes in different locations. If the inhibitor diffusivity is small enough then stable combinations of spikes are expected. Stable solutions should be possible for the following combinations: Type 1 multiple spikes only, Type 2 multiple spikes only, Type 3 multiple spikes only, combination of Type 2 and Type 3 multiple spikes. This would be in agreement with the case studies in the numerical computations (see Section 6).

The instabilities of the multiple spikes which we encountered in the numerical calculations were (i) disappearance of spikes when the amplitude becomes unstable (related to large eigenvalues) – this happens if the ratio of the diffusion constants $\frac{D}{\epsilon^2}$ is too large (ii) movement of the spikes to the boundary when their positions became unstable (related to small eigenvalues) – this occurs if D is too large. Such instabilities have been studied extensively for the standard Gierer–Meinhardt system and explicit stability thresholds have been established, see [29,30,35]. The same stability thresholds are also present for the system in this paper if one of the activators vanishes identically. It will be interesting to generalize the stability thresholds to the case that both activators are positive.

4. It will also be interesting to consider extensions of (1.1) for which the activators diffuse at different rates. We explored this issue numerically and found multiple spike solutions for u_1 and u_2, even if their diffusivities differ by some amount. However, the multiple spike solution converges to zero for large time if the diffusivities differ by too much.

In the simulations we computed (1.1) with $D = 0.01$, $\mu_1 = 1$, $\mu_2 = 3$, $\beta = 5$, $\tau = 0.1$, and initial conditions $u_i(x,0) = 0.4 + 0.2\cos(100 * \pi x)$ and $v(x,0) = 1.8 + 0.2\cos(100 * \pi x)$ for small diffusivities of the activators. First, the diffusivities for both activators were $\epsilon^2 = 0.0001$. Then we kept the diffusivity for u_1 fixed at 0.0001 but increased the diffusivity for u_2 to 0.0002, 0.0003, 0.0004. For the last case the multiple spikes are shown in Fig. 13.

Note that the spikes for u_2 are wider than for u_1 due to the larger diffusivity. If the diffusivity for u_2 is increased further to 0.0005, the solutions converge to the positive homogeneous steady state $(u_1, u_2, v) \approx (0.4142, 0.5858, 1.8873)$ for large time. It will be interesting to study the case of different diffusivities for the activators analytically.

CRediT authorship contribution statement

Weiwei Ao: Writing – original draft, Validation, Investigation, Conceptualization, Writing - review & editing, Methodology, Formal analysis, Resources, Funding acquisition. **Juncheng Wei:** Writing – original draft, Validation, Investigation, Conceptualization, Writing - review & editing, Methodology, Formal analysis, Resources, Funding acquisition. **Matthias Winter:** Writing – original draft, Validation, Investigation, Conceptualization, Writing – review & editing, Methodology, Formal analysis, Software, Visualization,.

Declaration of competing interest

The authors declare that they have no known competing financial interests or personal relationships that could have appeared to influence the work reported in this paper.

Acknowledgments

The work of W. Ao is supported by NSFC no. 12471111 and National key research and development program of China no. 2022YFA1006800. The research of J. Wei is partially supported by Hong Kong General Research Fund "New frontiers in singularity analysis of nonlinear partial differential equations". M. Winter thanks the Department of Mathematics at Wuhan University and the Department of Mathematics at Chinese University of Hong Kong for their kind hospitality.

Appendix

In this appendix we provide results from previous publications which are used repeatedly in the analysis.

The first result connects the eigenvalues for the limit problem and for the ϵ problem. In our context the ϵ problem is (4.1) with $\tau = 0$; the limit problem is (4.5), (4.6) for the two-activator spike solution and (4.15), (4.16) for the one-activator spike solution.

Theorem 1 of [43] can be reformulated as follows:

(i) If there is an eigenvalue λ for the limit problem with real part less than 1, then for ϵ small enough there is an eigenvalue λ_ϵ for the ϵ problem. On the other hand, if there are eigenvalues $\lambda_{\epsilon(n)}$ for a sequence $\epsilon(n) \to 0$ as $n \to \infty$, then there is a subsequence of $\epsilon(n)$ for which $\lambda_{\epsilon(n)}$ converges to a limit λ which is an eigenvalue of the limit problem.

(ii) If $B < 1$ and the limit problem has no eigenvalue with real part B, then the number of eigenvalues with real part less than B counting multiplicity is the same for the limit problem and the ϵ problem.

The second result explicitly states the eigenvalues for a nonlocal eigenvalue problem with cubic power nonlinearity.

Lemma 3.2 of [42]. *Consider the NLEP problem*

$$L_0\phi - cw^3 \int_{-\infty}^{\infty} w^2\phi\, dy = \lambda\phi, \quad -\infty < y < \infty; \quad \phi \to 0 \text{ as } |y| \to \infty,$$

for an arbitrary constant c corresponding to eigenfunctions for which $\int_{-\infty}^{\infty} w^2\Phi dy \neq 0$. Consider the range $Re(\lambda) > -1$, where $Re(\lambda)$ denotes the real part of λ. Then, on this range there is only one element in the point spectrum, and it is given explicitly by

$$\lambda = 3 - c\int_{-\infty}^{\infty} w^5\, dy.$$

The third result states the eigenspaces for a local eigenvalue problem with general power nonlinearity

Lemma 4.1 of [39] *The eigenvalue problem*

$$\Delta v - v + \mu v^{p-1}\phi = 0, \quad v \in H^1(\mathbb{R}^n)$$

admits a discrete set of eigenvalues $\nu_1 < \nu_2 \le \nu_3$ such that $\nu_1 = 1$, $\nu_i = p$, $2 \le i \le n+1$, and $\nu_{n+2} > p$. The eigenspaces V_1 and V_p corresponding to 1 and p, respectively, are given by

$$V_1 = span\{w\}$$

and

$$V_p = span\left\{\frac{\partial w}{\partial x_i} \mid 1 \le i \le n\right\}.$$

The final result gives estimates of the eigenvalues for a local eigenvalue problem.

Theorem 4.1 of [11] *(3) If $\mu_R > 0$, then the eigenvalue problem*

$$\phi'' - \phi + (1+\mu_R)w^{p-1}\phi = \lambda\phi, \quad \phi \in H^1(\mathbb{R})$$

admits a positive (principal) eigenvalue λ_1 such that

$$-\lambda_1 = \inf_{\phi\in H^1(\mathbb{R})\setminus\{0\}} \frac{\int_{-\infty}^{\infty}[(\phi')^2 + \phi^2 - (1+\mu_R)w^{p-1}\phi^2]\, dy}{\int_{-\infty}^{\infty}\phi^2\, dy.}$$

(4) Let ϕ (complex-valued) satisfy the following eigenvalue problem

$$\begin{cases} \phi'' - \phi + w^{p-1}\phi + (p-1)\sigma w^{p-1}\phi = \lambda\phi, \\ \mathrm{Re}(\sigma) \le 0, \quad \phi \in H^1(\mathbb{R}), \quad \lambda \neq 0. \end{cases}$$

Then $\mathrm{Re}(\lambda) < 0$.

Data availability

Data will be made available on request.

References

[1] A. Gierer, H. Meinhardt, A theory of biological pattern formation, Kybern. (Berlin) 12 (1972) 30–39.
[2] C. Kratochwil, R. Mallarino, Mechanisms underlying the formation and evolution of vertebrate color patterns, Annu. Rev. Genet. 57 (2023) 135–156.
[3] M. Hirata, K.-I. Nakamura, S. Kondo, Pigment cell distributions in different tissues of the zebrafish, with special reference to the striped pigment pattern, Dev. Dyn. 234 (2005) 293–300.
[4] C. Nüsslein-Volhard, A.P. Singh, How fish color their skin: A paradigm for development and evolution of adult patterns: Multipotency, plasticity, and cell competition regulate proliferation and spreading of pigment cells in zebrafish coloration, Bioessays 39 (2017) 1600231.
[5] J. Teyssier, S.V. Saenko, D. van der Marel, M.C. Milinkovitch, Photonic crystals cause active colour change in chameleons, Nat. Commun. 6 (2015) 6368.
[6] A. Volkening, B. Sandstede, Modelling stripe formation in zebrafish: An agent-based approach, J. R. Soc. Interface 12 (2015) 20150812.
[7] A. Volkening, B. Sandstede, Iridophores as a source of robustness in zebrafish stripes and variability in Danio patterns, Nat. Commun. 9 (2018) 3231.
[8] M.R. McGuirl, A. Volkening, B. Sandstede, Topological data analysis of zebrafish patterns, Proc. Natl. Acad. Sci. 117 (2020) 5113–5124.
[9] C. Gai, T. Kolokolnikov, Resource-mediated competition between two plant species with different rates of water intake, SIAM J. Appl. Math. 83 (2023) 576–602.
[10] J. Wei, M. Winter, On a two-dimensional reaction–diffusion system with hypercyclical structure, Nonlinearity 13 (2000) 2005–2032.
[11] J. Wei, M. Winter, On a hypercycle system with nonlinear rate, Methods Appl. Anal. 8 (2001) 257–277.
[12] J. Wei, M. Winter, Critical threshold and stability of cluster solutions for large reaction–diffusion systems in R^1, SIAM J. Math. Anal. 33 (2002) 1058–1089.
[13] J. Wei, M. Winter, Mutually exclusive spiky pattern and segmentation modeled by the five-component Meinhardt-Gierer system, SIAM J. Appl. Math. 69 (2008) 419–452.
[14] M. Eigen, P. Schuster, The Hypercycle: A Principle of Natural Selforganisation, Springer, Berlin, 1979.
[15] H. Meinhardt, A. Gierer, Generation and regeneration of sequences of structures during morphogenesis, J. Theoret. Biol. 85 (1980) 429–450.
[16] H. Meinhardt, Models of Biological Pattern Formation, Academic Press, London, 1982.
[17] T.-C. Lin, J. Wei, Ground state of N coupled nonlinear Schrödinger equations in R^n, $n \le 3$, Comm. Math. Phys. 255 (2005) 629–653.
[18] T.-C. Lin, J. Wei, Spikes in two coupled nonlinear Schrödinger equations, Ann. Non Linearie Ann. de L'Inst. H. Poincare 22 (2005) 403–439.
[19] T.-C. Lin, J. Wei, Spikes in two-component systems of nonlinear Schrödinger equations with trapping potentials, J. Differential Equations 229 (2006) 538–569.
[20] T.-C. Lin, J. Wei, Solitary and self-similar solutions of two-component system of nonlinear Schrödinger equations, Phys. D 220 (2006) 99–115.
[21] T.-C. Lin, J. Wei, Symbiotic bright solitary wave solutions of coupled nonlinear Schrödinger equations, Nonlinearity 19 (2006) 2755–2773.
[22] T.-C. Lin, J. Wei, Orbital stability of bound states of semi-classical nonlinear Schrödinger equations with critical nonlinearity, SIAM J. Math. Anal. 40 (2008) 365–381.

[23] J. Wei, W. Yao, Uniqueness of positive solutions to some coupled nonlinear Schrödinger equations, Comm. Pure Appl. Anal. 11 (2012) 1–9.
[24] E.N. Dancer, J. Wei, Spike solutions in coupled nonlinear Schrödinger equations with attractive interaction, Trans. Amer. Math. Soc. 361 (2009) 1189–1208.
[25] J. Wei, M. Zhen, Classification of positive ground state solutions with different Morse indices for nonlinear N-coupled Schrödinger system, Anal. Theory Appl. 37 (2021) 230–266.
[26] E.N. Dancer, J. Wei, T. Weth, A priori bounds versus multiple existence of positive solutions for a nonlinear Schrödinger system, Ann. Inst. H. Poincaré Anal. Non Linéaire 27 (2010) 953–969.
[27] A.M. Turing, The chemical basis of morphogenesis, Phil. Trans. Roy. Soc. Lond. B 237 (1952) 37–72.
[28] A. Doelman, R.A. Gardner, T.J. Kaper, Stability analysis of singular patterns in the 1D Gray-Scott model: A matched asymptotics approach, Phys. D 122 (1998) 1–36.
[29] A. Doelman, R.A. Gardner, T.J. Kaper, Large stable pulse solutions in reaction–diffusion equations, Indiana Univ. Math. J. 50 (2001) 443–507.
[30] D. Iron, M. Ward, J. Wei, The stability of spike solutions to the one-dimensional Gierer-Meinhardt model, Phys. D 50 (2001) 25–62.
[31] M.J. Ward, J. Wei, Hopf bifurcations and oscillatory instabilities of spike solutions for the one-dimensional Gierer-Meinhardt model, J. Nonlinear Sci. 13 (2003) 209–264.
[32] J. Wei, M. Winter, On the two-dimensional Gierer-Meinhardt system with strong coupling, SIAM J. Math. Anal. 30 (1999) 1241–1263.
[33] J. Wei, M. Winter, Spikes for the two-dimensional Gierer-Meinhardt system: The weak coupling case, J. Nonlinear Sci. 11 (2001) 415–458.
[34] J. Wei, M. Winter, Spikes for the two-dimensional Gierer-Meinhardt system: The strong coupling case, J. Differential Equations 178 (2002) 478–518.
[35] J. Wei, M. Winter, Existence, classification and stability analysis of multiple-peaked solutions for the Gierer-Meinhardt system in R, Methods Appl. Anal. 14 (2007) 119–164.
[36] J. Wei, M. Winter, Mathematical Aspects of Pattern Formation in Biological Systems, Vol. 189, Springer Science & Business Media, London, 2013.
[37] D. Gilbarg, N.S. Trudinger, Elliptic Partial Differential Equations of Second Order, in: Grundlehren Math. Wiss., vol. 224, Springer, Berlin Heidelberg New York, 1983.
[38] C. Gui, J. Wei, Multiple interior peak solutions for some singular perturbation problems, J. Differential Equations 158 (1999) 1–27.
[39] J. Wei, On the construction of single-peaked solutions to a singularly perturbed semilinear Dirichlet problem, J. Differential Equations 129 (1996) 315–333.
[40] J. Wei, M. Winter, Stationary solutions for the Cahn-Hilliard equation, Ann. Inst. H. Poincaré Anal. Non Linéaire 15 (1998) 459–492.
[41] J. Wei, On single interior spike solutions of Gierer-Meinhardt system: Uniqueness, spectrum estimates and stability analysis, Euro. J. Appl. Math. 10 (1999) 353–378.
[42] T. Kolokolnikov, M.J. Ward, J. Wei, The stability of steady-state hot-spot patterns for a reaction–diffusion model of urban crime, Discrete Contin. Dyn. Syst. Ser. B 19 (2014) 1373–1410.
[43] E.N. Dancer, On stability and Hopf bifurcations for chemotaxis systems, Methods Appl. Anal. 8 (2001) 245–256.